OUTP-15-aaP

The PDF4LHC report on PDFs and LHC data: Results from Run I and preparation for Run II

The PDF4LHC Working Group: Juan Rojo[1], Albert de Roeck (eds.), Richard D. Ball, Amanda Cooper-Sarkar[2], Stephen Farry, Joey Huston, Maxime Gouzevitch[3], Claire Gwenlan[2], Katerina Lipka, Pavel Nadolsky, Robert Thorne, ...

[1] *Rudolf Peierls Centre for Theoretical Physics, University of Oxford, 1 Keble Road, Oxford OX1 3NP, United Kingdom*

[2] *Particle Physics, Department of Physics, University of Oxford, 1 Keble Road, Oxford OX1 3NP, United Kingdom*

[3] *Université de Lyon, Université Claude Bernard Lyon 1, CNRS-IN2P3, Institut de Physique Nucléaire de Lyon, Villeurbanne, France*

Abstract

The accurate determination of the Parton Distribution Functions (PDFs) of the proton is an essential ingredient of the Large Hadron Collider (LHC) program. PDF uncertainties impact a wide range of processes, from Higgs boson characterization and precision Standard Model measurements, to New Physics searches. A major development in modern PDF fits has been the inclusion of a wealth of measurements from the LHC. In this report we summarise the information that PDF-sensitive measurements at the LHC Run I have provided, and then we review the prospects for the corresponding measurements at Run II. We also present an overview of those studies that have quantified the information on PDFs provided by LHC data. This document should provide useful input to the LHC collaborations to prioritize their PDF-sensitive measurements at Run II, and will also provide a comprehensive set of references for the PDF fitting collaborations.

Contents

1 Introduction and motivation **3**

2 PDF analysis at the dawn of the LHC Run II **5**
2.1 CT14 . . . 5
2.2 MMHT14 . . . 6
2.3 NNPDF3.0 . . . 7
2.4 HERAPDF . . . 7
2.5 ABM12? . . . 8
2.6 PDF comparison plots . . . 8

3 Overview of PDF-sensitive measurements at the LHC **11**
3.1 Jet production . . . 11
3.2 Prompt photon production . . . 12
3.3 Inclusive W and Z production and asymmetries . . . 13
3.4 High and low mass Drell-Yan production . . . 13
3.5 The transverse momentum of W and Z bosons . . . 14
3.6 W production in association with charm quarks . . . 14
3.7 Top quark pair production . . . 15
3.8 Charm and bottom pair production . . . 16
3.9 Central exclusive production . . . 16
3.10 Ratios of cross-sections for different center-of-mass energies . . . 16

4 Constraining PDFs with LHC data at Run I **18**
4.1 Constraints from ATLAS . . . 18
4.2 Constraints from CMS . . . 21
4.3 Constraints from LHCb . . . 24

5 Prospects for Run II measurements **26**
5.1 Prospects from ATLAS . . . 26
5.2 Prospects from CMS . . . 27
5.3 Prospects from LHCb . . . 28

6 Summary and outlook **30**

1 Introduction and motivation

The initial state of hadronic collisions is the domain of the parton distribution functions (PDFs) of the proton (see for example [1–6] for recent reviews). PDFs are an essential ingredient for LHC phenomenology: they limit the accuracy with which it is possible to extract the Higgs boson couplings from the LHC measurements [5, 7], degrade the reach of searches for massive new BSM particles at the TeV scale [8, 9] and are the dominant systematic uncertainty in the determination of fundamental parameters such as the W boson mass or $\sin^2\theta_{\rm eff}$, that are key ingredients for global stress-tests of the Standard Model [10–12]. Being non-perturbative objects, although their scale dependence is determined by the perturbative DGLAP evolution equations, they need to be extracted from global fits to hard-scattering data. Various PDF fitting collaborations provide regular updates of their QCD analysis, some of the latest PDF releases include ABM12 [13], CT14 [14], HERAPDF2.0 [15], MMHT14 [16] and NNPDF3.0 [17].

A major recent development in PDF fits has been the inclusion of a wide variety of LHC data. Some of the LHC processes that are now used in PDF fits were already part of global PDF fits, for example using Tevatron measurements, but now LHC data opens a wider new kinematical ranges, for instance for jet production [18–20] and for inclusive electroweak boson production [21, 22]. On the other hand, other types of processes have only become become available for PDF fits after their measurement at the LHC, like isolated direct photon production [23], W production in association with charm quarks [24–26], top quark pair production [27, 28], open charm and bottom production [29, 30], low and high mass Drell-Yan production [31, 32] and W and Z production in association with jets [33], among many others. Remarkably, some of these processes open completely new avenues for PDF fits, for instance data on $W+c$ production provides a clean handle on the strange PDF $s(x, Q^2)$ [24–26, 34] complementary to that of the low energy neutrino data [35], and top quark pair production allows constraints on the large-x gluon complementary to jets [27, 28, 36].

The fact that the LHC provides measurements at different center-of-mass energies also allows to construct novel observables with useful PDF sensitivity [37], the ratios and double ratios of cross-sections at different values of $\sqrt{s}$ where many theoretical and experimental uncertainties cancel. This concept has already been validated by measurements such as ATLAS analysis of the ratio of jet cross-sections between 7 and 2.76 TeV [19] and the CMS measurement of the ratio of Drell-Yan cross-sections between 8 and 7 TeV [38], and many more related ratios will be measured at Run II between 13 and 8 TeV. Another important example of the relevance of LHC data for parton distributions is given by close interplay PDFs and the tunes of soft and semi-hard QCD models in the context of LO and NLO event generators, where LHC measurements has been shown to provide invaluable constraints on these models [39, 40]. Finally, PDFs are an irreducible background to the extraction of Standard Model parameters at the LHC, for instance the recent direct measurements of the strong coupling in the TeV regime [41, 42].

Another important development for PDF studies in the recent years has been the availability of PDF fits being carried out also the ATLAS and CMS collaborations themselves. Thanks to the know-how acquired from the HERA data analysis, and the availability of a public tool for PDF fits like HERAFITTER [43], both collaborations have developed an extensive program of PDF determinations from their own measurements [19, 21, 22, 41].

The aim of these studies is not to provide an alternative to global fits, both rather to study internally the constraints on their own measurements of PDFs prior to publication, ensure that all information in correlated systematics is suitably provided and to perform checks of the data prior to publication using the QCD analysis as a diagnosis toolbox.[1]

Given the importance that LHC data has now in global PDF fits, and the upcoming restart of the LHC at 13 TeV, it is now timely to summarize what have we learned for PDFs from Run I data, and to set the stage for the corresponding measurements at Run II. Therefore, the aim of this document is to review the constraints on PDFs that measurements at the Large Hadron Collider during the Run I data-taking have provided. With this motivation, we summarize the various measurements from ATLAS, CMS and LHCb that can be used to provide constraints into PDFs, and discuss the available phenomenological studies that quantify the information on PDFs provided by these LHC datasets. Then we move to discuss the prospects for PDF-sensitive data at the upcoming Run II at 13 TeV. We explore how the increase in center of mass energy and luminosity can provide new opportunities for PDF studies beyond those available at Run I.

The outline of this document is the following. First of all, in Sect. 2 we summarize the status of the latest PDF releases from the main fitting collaborations, with emphasis on the role that LHC data has on these. Then in Sect. 3 we present a overview of those recent studies that have quantified the PDF sensitivity of LHC measurements. We continue in Sect. 4 with a more detailed summary of the relevant measurements and their corresponding constraints on PDFs that the ATLAS, CMS and LHCb collaborations have provided at Run I. Next, in Sect. 5, we have a discussion about the prospects for PDF-sensitive measurements at Run II. We conclude in Sect. 6 with an outlook on the program of constraining PDFs with LHC data for the coming years.

This report summarizes the discussions that have taken place at various forums, in particular at the regular PDF4LHC meetings, during the last months. It is also indebted to the productive discussions that took place at the *"Parton Distributions for the LHC"* workshop that took place between the 15th and the 22nd of February 2015 at the Benasque Center for Science *Pedro Pascual*.[2]

Let us also mention that in parallel with the studies summarized in these report, an update of the benchmark comparisons between different PDF groups, as well as between different possible methods to combine them [46], is also being performed, with the aim of updating the current PDF4LHC recommendations [47,48] about the PDF usage at the LHC Run II. The results of these benchmark comparisons will be presented separately in a companion publication.

[1] In addition, the HERAFITTER developers are also performing a number of independent PDF studies [44,45].

[2] `http://benasque.org/2015lhc/`

2 PDF analysis at the dawn of the LHC Run II

We begin this document with a succinct review of the status of PDF fits at the dawn of the Run II of the LHC. This is specially relevant since most PDF groups have provided major updates of their fits in time to be used with the Run II data taking, data analysis and Monte Carlo generation. In this section we summarize the recent developments of these various groups. We emphasize the role that LHC data plays on each of these analysis. The reader is encouraged to consult the original publications for additional information about these updated PDF fits. It is beyond the scope of this work to provide a detailed comparison between these updated sets, so here we restrict ourselves to a subset of comparisons between PDFs and their luminosities using the APFEL-Web interface [49, 50].

2.1 CT14

CT14 provides parton distribution functions at LO, NLO and NNLO. The global PDF fits include LHC data for the first time, from ATLAS, CMS and LHCb, to go along with the data sets used for CT10. One important, recently released data set from the Tevatron has also been added, that of the D0 W muon asymmetry measurement using the full Run 2 data sample. This data set provides important constraints on u and d quarks at high x, and on $\bar{u}$ and $\bar{d}$ quarks at low x. The LHC data sets chosen for the global fits are those for which NNLO predictions are available and which are expected to provide additional constraints on PDFs in regions applicable for LHC physics analyses. An exception is made for measurements of the inclusive jet cross section, where the complete NLO calculation is not yet available. However, the corrections determined for the gg initial state are reasonably small and flat as a function of the jet transverse momentum and the expectation is that the same will be true for the other initial states.

There are a total of 3045 data points included from 35 experiments. fastNLO and applgrid interfaces have been used for quick calculations of NLO matrix elements in the global fits, supplemented by NNLO K-factors (for the NNLO fit). ResBos has been used for the calculation of the NNLO K-factors for W/Z and W asymmetry data.

The PDF parametrization is more flexible than that of CT10.The PDFs are expressed as a linear combination of Bernstein polynomials, where each basis polynomial has a single peak. This serves to reduce any correlations among the parameters. PDF error sets with a total of 27 eigenvectors are provided at both NLO and NNLO. A central value of

$\alpha_s(m_Z)$ of 0.118 has been assumed in the global fits at NLO and NNLO, but PDF sets at alternate values of $\alpha_s(m_Z)$ are also provided. As with the CTEQ6 leading order PDFs, two versions are supplied, one with a 1-loop $\alpha_s(m_Z)$ value of 0.130 and the other with a 2-loop $\alpha_s(m_Z)$ value of 0.118.

In general, the CT14 PDFs are similar to those from CT10, albeit with a somewhat smaller strange quark distribution at low x and a somewhat softer gluon at high x. Furthermore, CT14 and CT10 differ in the u and d quark distributions at moderate to large x, due to the inclusion of new data, both from the LHC and from the Tevatron. Particular attention is paid to the behavior of the d/u ratio in the limit as x approaches 1. The CT14 parameterization assumes that

d_v/u_v approaches a constant as $x \to 1$, by assuming that $u_v(x)$ and $d_v(x)$ both vary as $(1-x)^{a2}$, with the same value of $a2$ for both (but allowing for different normalizations).

This is consistent with the expectations of spectator counting rules.

2.2 MMHT14

The MMHT2014 PDF sets were released in December 2015 [16]. They are the first major update based on this framework since the MSTW2008 PDFs [51]. However, the updates incorporate the improvements to the parametrisation and deuteron corrections already presented in Ref. [52]. This study showed that the new parameterizations, which use Chebyshev polynomials in $(1-2\sqrt{x})$ rather than simple powers of $\sqrt{x}$ and up to 7 free parameters for a particular PDF, can reproduce functions obtained from a much greater number of parameters up to a small fraction of percent over a wide range in x. The more flexible deuteron corrections improve the fit quality and result in a shape similar to the models in e.g. [53]. The new PDF sets also use the optimal variable flavour number scheme of [54], updated heavy nucleus corrections [55], a modified uncertainty central value and uncertainty for the branching ratio $B_\mu = B(D \to \mu)$ used in the determination of the strange quark from dimuon data, and use the multiplicative rather than additive definition for correlated systematic uncertainties [56].

The data used in the fits have been very significantly updated from the MSTW2008 analysis, with relevant data sets published before the beginning of 2014 included. In particular the combined HERA total cross section data [57] and combined charm data [58] are now used, along with some updates on Tevatron W production. Moreover, a variety of LHC data, including W, Z and $\gamma^\star$ data from ATLAS, CMS and LHCb, inclusive jet data from ATLAS and CMS and total top pair production from ATLAS and CMS (and the Tevatron combined result [59]) have now been included. A summary is found in Sect. 3. Although they have not been used to determine the PDFs, data on $W + c$ production and differential top pair production have been checked against the PDFs and give good agreement. NLO calculations are produced for LHC data using [41-42] and K-factors employed at NNLO. The LHC inclusive jet data are currently not used at NNLO, leading to a very slight increase in the uncertainty for the high-x gluon at NNLO compared to NLO.

The resulting PDFs are made available with a best fit set and 25 68% confidence level eigenvector pairs at LO, NLO and NNLO and corresponding to $\alpha_S(M_Z^2)$ values of 0.130 at LO, 0.118 and 0.120 at NLO and 0.118 at NNLO. The increase in the number of eigenvectors from 20 in the MSTW2008 sets is due to the increased flexibility of the PDFs, partially made possible by extra constraints coming from new LHC data types. The $\alpha_S(M_Z^2)$ is left free in fits in the first instance, result in best fits near 0.135 at LO, 0.120 at NLO and 0.118 at NNLO. Hence the choice of the values for the eigenvector sets, though 0.118 is available as well as 0.120 at NLO since this is near the world average for $\alpha_S(M_Z^2)$, and a set with this value may be required by users. Each eigenvector set is accompanied by a central set with $\alpha_S(M_Z^2)$ values with ± 0.001 in order to enable uncertainties due to $\alpha_S(M_Z^2)$ to be calculated.

Sets with a wide variety of $\alpha_S(M_Z^2)$ values have been determined and will be made available very soon and followed by sets with a variety of values of charm and bottom mass, and in the three and four flavour schemes. The MMHT2014 PDFs generally give very similar results for LHC observables as the MSTW2008 PDFs, and have comparable uncertainties. The main change in the MMHT2014 PDFs is in the small-x valence quarks,

and is due to the improved parameterisation and deuteron corrections, and an increase in the uncertainty (and to a lesser extent the central value) of the strange quark. The latter is due to the quite generous uncertainty allowed on $B_\mu = B(D \to \mu)$ and an extra free parameter for the strange quark contributing to the eigenvectors. This combination of extra freedom in the strange PDF is then given an extra constraint by the LHC W and Z boson production data.

2.3 NNPDF3.0

The NNPDF3.0 sets were released in October 2014 [17]. As compared to its predecessor, NNPDF2.3 [60], NNPDF3.0 is the result of a extensive development of the NNPDF fitting machinery, in terms of new experimental constraints, theoretical calculations, code organization and methodology. All the fitting code has been rewritten from FORTRAN to C++ and PYTHON, making it really robust and modular, so that the addition of new experiments or the modification of the theoretical calculations can be done easily with almost no need to modify the code. For the experimental data point of view, NNPDF3.0, as compared to NNPDF2.3, includes all the published HERA-II data from H1 and ZEUS, and a wide range of ATLAS, CMS and LHCb data on jet production, weak boson production and asymmetries, Drell-Yan, W+charm and top quark pair production. The complete list of LHC measurements that have been included in NNPDF3.0 will be summarized in Sect. 4.

Concerning theory calculations, all collider processes have been computed using fast NLO interfaces [61–63], supplemented by NNLO and electroweak K-factors when required. Inclusive jets are included at NNLO using the approximate threshold resummation [64,65], validated on the exact calculation on the gg channel [66]. DIS structure functions are as usual computed in the FONLL General-Mass variable-flavor number scheme [67], with the main difference being that at NLO it is the FONLL-B scheme that is used, rather than FONLL-A as previously, since it allows a better description of the low Q^2 charm production data. The fitting methodology is based on closure tests with artificial pseudo-data, which allows to cleanly separate the different contributions to the total PDF uncertainty, as well as to verify the statistical interpretation of PDF uncertainties as genuine 68% confidence level ranges.

2.4 HERAPDF

The HERAPDF fits are based only on data collected at the HERA ep collider. During HERA-I and HERA-II running approximately $1 fb^{-1}$ of data were collected divided roughly equally between e^+p and e^-p scattering. All of the published measurements on inclusive Neutral and Charged Current (NC and CC) scattering have now been combined into a single coherent data set taking into account correlated systematic uncertainties [68]. This combination includes data taken at different proton beam energies, $E_p = 920, 820, 575, 460$ GeV. The data cover the ranges $6 \times 10^{-7} < x < 0.65$, $0.045 < Q^2 < 50,000$ GeV^2. The combination led to significantly reduced uncertainties, below 1.5% over the kinematic range $3 < Q^2 < 500$ GeV^2. This combination supersedes the previous combination of only HERA-I data.

The availability of precision NC and CC data over such a large kinematic range allows the extraction of PDFs using only ep data without the need for heavy target corrections.

The difference between the NC e^+p and e^-p cross sections at high Q^2 constrains the valence PDFs. The high-x CC data separate valence quark flavours. The CC e^-p data allow the extraction of the d-valence PDF without assuming strong isospin symmetry. The lower-Q^2 NC data constrain the sea PDF directly and through their scaling violations they constrain the gluon PDF. A further constraint on the gluon comes from the data at different beam energies, which probe the longitudinal structure function F_L. The HERAPDF2.0 is based on the new data combination [68] and supersedes HERAPDF1.0 and 1.5 which were based on previous partial combinations. The HERAPDF2.0 is available at LO, NLO and NNLO on `LHAPDF6`. The experimental uncertainties are presented as 14 pairs of Hessian eigenvectors evaluated by the standard criterion of $\Delta\chi^2 = 1$. For the NLO and NNLO PDFs 13 further variations are supplied to cover uncertainties due to model assumptions and assumptions on the form of the parametrisation. For the NLO and NNLO PDFs the standard value of $\alpha_S(M_Z) = 0.118$ but the PDFs are also supplied for values of $0.110 < \alpha_S(M_Z) < 0.130$ in steps of 0.001.

Several further variations of the HERAPDF2.0 are also supplied: HERAPDF2.0HiQ2 for which only data with $Q^2 > 10$ GeV^2 are used to avoid possible bias from low-x, low-Q^2 effects; HERAPDF2.0AG for which the gluon takes form which is imposed to be positive definite for all x for which $Q^2 > 3.5$ GeV^2; HERAPDF2.0FF3A and FF3B, which use two different versions of the Fixed Flavour Number Scheme for heavy quarks; and finally HERAPDF2.0Jets which uses additional HERA data on jet production as well as the HERA combined charm data. The charm data mostly serve to constrain the uncertainty on the charm quark mass parameter and this information is already used in the main HERAPDf2.0 PDFs, whereas the jet data put further constraints on the gluon PDF, such that a simultaneous fit for $\alpha_S(M_Z)$ and the PDFs can be made, resulting in a competitive determination of $\alpha_S(M_Z)$.

Let us also mention that this legacy HERA combination is expected to become the basis for all future fits to LHC data that are performed using the `HERAfitter` framework.

2.5 ABM12?

2.6 PDF comparison plots

To conclude this section, we provide some plots to compare the latest releases from the various PDF collaborations. We provide comparisons at the level of PDFs, and then also we perform a comparison of the PDF luminosities. To begin with, we show some comparison plots between the NNPDF3.0, CT14 and MMHT14 NNLO sets.[3] In all these comparison plots, the APFEL-Web interface [49, 50] has been used.

First of all we compare PDF luminosities at the LHC with a center of mass energy of 13 TeV, the results are shown in Fig. 1. As compared to previous benchmark studies, we see an improved convergence between the three sets in a number of phenomenologically important regions, like the gg luminosity at intermediate values of the final state invariant mass M_X. For the four luminosities that are shown here, gg, qq, $q\bar{q}$ and gg, the three sets agree at the one-sigma level or better. The differences are larger at large invariant masses, a key region for massive New Physics searches at the LHC, where also the intrinsic

[3] We use here a preliminary version of the CT14NNLO set, provided by P. Nadolsky, which should be very close to the final version.

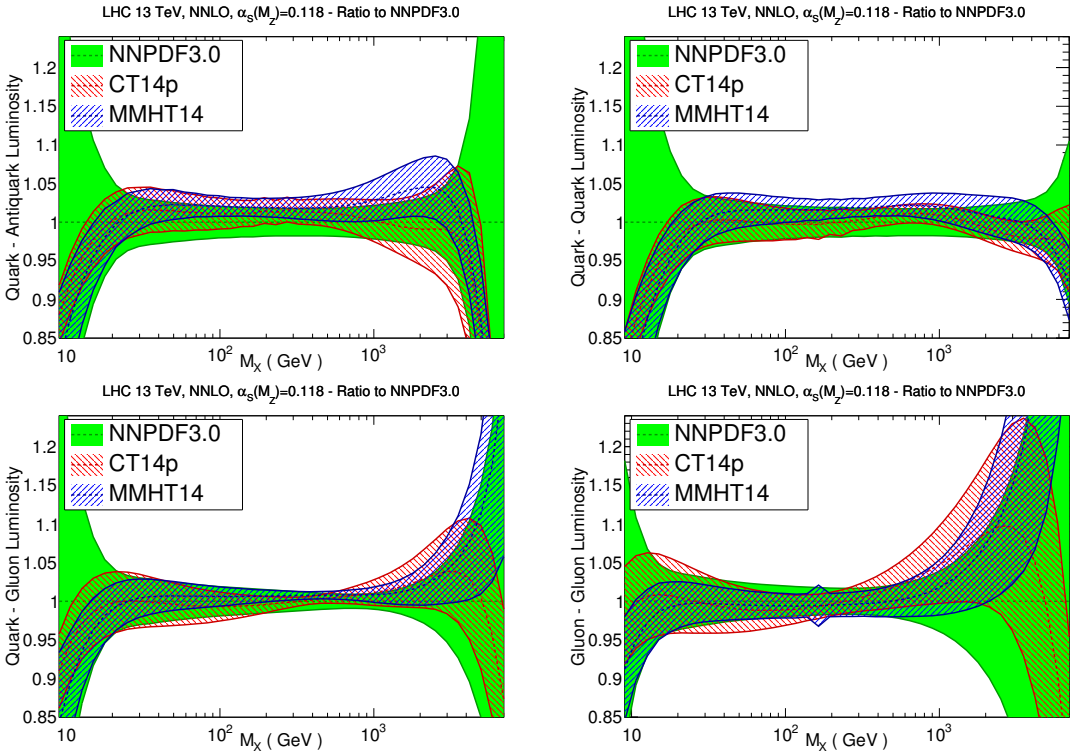

Figure 1: Comparison of PDF luminosities between NNPDF3.0, MMHT14 and CT14p. The comparison has been performed at NNLO for the LHC with a center of mass energy of 13 TeV, as a function of the invariant mass of the final state system. Results are shown normalized to the central value of the NNPDF3.0 NNLO set.

PDF uncertainties for each group are rather substantial due to the lack of experimental constraints.

Now we turn to the corresponding comparison of the PDFs at a low scale, $Q_0^2 = 2$ GeV^2 between NNPDF3.0, CT14p and MMHT14, all of them at NNLO. From top to bottom, and from left to right, we show the gluon, the total quark singlet, the total valence, and the strangeness PDFs. We see reasonable agreement at the level of one-sigma, with some marked differences in the sizes of the PDF uncertainties specially in the extrapolation region at small-x.

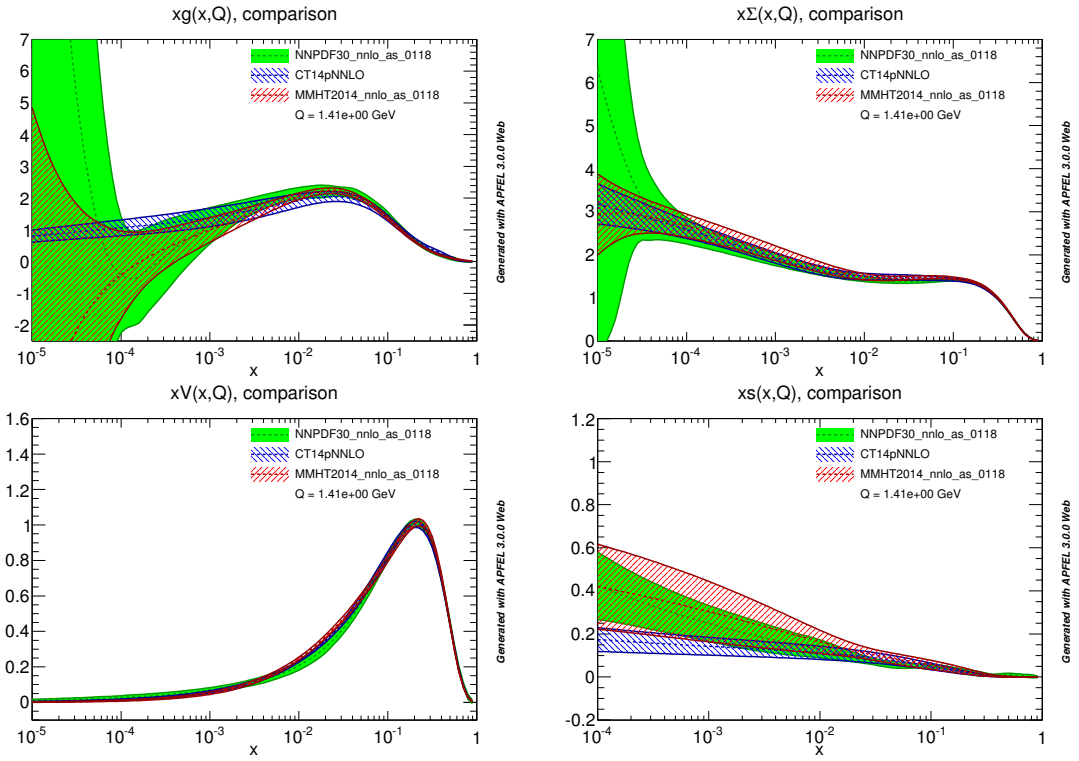

Figure 2: Comparison of PDFs at $Q_0^2 = 2$ GeV^2 between NNPDF3.0, CT14p and MMHT14, all of them at NNLO. From top to bottom, and from left to right, we show the gluon, the total quark singlet, the total valence, and the strangeness PDFs. All plots have been obtained using the APFEL-Web online plotting interface.

3 Overview of PDF-sensitive measurements at the LHC

As we have mentioned in the introduction, at the LHC a rich variety of observables can be used for PDF constraints. In this section, we would like to perform a general overview of those LHC processes, with emphasis on the new information that they provide on top of existing processes in PDF fits, as well as a brief summary of the range of Bjorken-x, of Q^2 and of the PDF flavors that they are most sensitive to. In other words, in this section we provide the generic motivation for the measurement of specific processes at the LHC to be used in PDF analysis. When available, the actual measurements that have been performed by ATLAS, CMS and LHCb are presented in the next section. Likewise, we leave for the next section the exact list of which LHC measurements have been used in which PDF fits up to now, trying to keep the discussion here as light and self-contained as possible. We also include here those measurements that have been proposed as good candidates to provide information in PDF fits, but that have yet not been measured or made available in a format suitable for PDF studies.

3.1 Jet production

Jet production allows to constrain quarks and gluons at medium and large-x [69], the latter in a range which is not covered by deep-inelastic scattering data. Inclusive jet production has been used in PDF fits since the first measurements at the Tevatron, and now from the LHC a number of precise inclusive jets, dijets and three jet measurements have become available for their use in PDF fits. In addition, let us mention that jet production provides a unique possibility for direct determinations of the strong coupling $\alpha_S(Q)$ in the TeV range way above any other existing measurements, information on BSM physics.

Jet production can be presented in a different number of complementary ways, the most traditional are the measurements of the inclusive jet and dijet cross-sections, but measurements of three-jet and multi-jet cross-sections have also became available recently. The impact of ATLAS and CMS jet data into PDFs has been quantified in a number of studies, both from global PDF fitting groups [17, 18] and from the LHC collaborations themselves [19, 41]. In addition to the large-x gluon, also information on the large-x quarks can be obtained, since at the highest values of the jet transverse momentum is the quark-quark scattering mechanism that dominates, due to the steeper fallout of the gluon PDF at large-x.

While the NLO calculation for inclusive and dijet production has been available for more than 20 years, only recently the first partial results on the NNLO calculation have become available [66, 70]. It is expected that the full NNLO results will have a substantial impact on the analysis of the LHC data in the context of PDF fits. While the full calculation is available, it has been proposed that a subset of jet data can still be consistently included in NNLO fits by using the approximate NNLO threshold calculation. This strategy, presented in [65] has been used for example to include LHC jet data in the NNPDF3.0 NNLO fit.

REACTION	OBSERVABLE	PDFS	x	Q
$pp \to W^{\pm} + X$	$d\sigma(W^{\pm})/dy_l$	$q, \bar{q}$	$10^{-3} \lesssim x \lesssim 0.7$	$\sim M_W$
$pp \to \gamma^*/Z + X$	$d^2\sigma(\gamma^*/Z)/dy_{ll}dM_{ll}$	$q, \bar{q}$	$10^{-3} \lesssim x \lesssim 0.7$	5 GeV $\lesssim Q \lesssim$ 2 TeV
$pp \to \gamma^*/Z + \text{jet} + X$	$d\sigma(\gamma^*/Z)/dp_T^{ll}$	q, g	$10^{-2} \lesssim x \lesssim 0.7$	200 GeV $\lesssim Q \lesssim$ 1 TeV
$pp \to \text{jet} + X$	$d\sigma(\text{jet})/dp_T dy$	q, g	$10^{-2} \lesssim x \lesssim 0.8$	20 GeV $\lesssim Q \lesssim$ 3 TeV
$pp \to \text{jet} + \text{jet} + X$	$d\sigma(\text{jet})/dM_{jj}dy_{jj}$	q, g	$10^{-2} \lesssim x \lesssim 0.8$	500 GeV $\lesssim Q \lesssim$ 5 TeV
$pp \to t\bar{t} + X$	$\sigma(t\bar{t}), d\sigma(t\bar{t})/dM_{t\bar{t}}$, ...	g	$0.1 \lesssim x \lesssim 0.7$	350 GeV $\lesssim Q \lesssim$ 1 TeV
$pp \to c\bar{c} + X$	$d\sigma(c\bar{c})/dp_{T,c}dy_c$	g	$10^{-5} \lesssim x \lesssim 10^{-3}$	1 GeV $\lesssim Q \lesssim$ 10 GeV
$pp \to b\bar{b} + X$	$d\sigma(b\bar{b})/dp_{T,c}dy_c$	g	$10^{-4} \lesssim x \lesssim 10^{-2}$	5 GeV $\lesssim Q \lesssim$ 30 GeV
$pp \to W + c$	$d\sigma(W + c)/d\eta_l$	$s, \bar{s}$	$0.01 \lesssim x \lesssim 0.5$	$\sim M_W$

Table 1: Summary of some of the LHC processes with sensitivity to PDFs discussed in this section. For each process, we quote the corresponding measured distribution, the PDFs that are probed, and the approximate ranges of x and Q^2 that can be accessible using available Run I data. These ranges have been obtained assuming the Born kinematics, as in Ref. [71]. This table is just for illustration purposes and thus is not necessarily exhaustive.

3.2 Prompt photon production

Direct photon production from fixed-target experiments was recognized as a useful probe of the gluon PDFs a long time ago, but at some photon data stop being used both because of the availability of Tevatron jet data and some inconsistencies between different fixed-target measurements. More recently, the use of LHC isolated photon data back into PDF fits was advocated in Ref. [23], where a reanalysis of all available fixed target and collider isolated direct photon production data was performed, finding good consistency with NLO QCD calculations. In Ref. [23] it was also shown that direct photon data can potentially constrain the gluon PDF in a intermediate range of x, $x \sim 0.01$, which is the region relevant for Higgs boson production via gluon fusion. The main obstacle for the full inclusion of direct photon data into PDF fits is the large scale uncertainties that affect the NLO QCD calculation. The possibility to use isolated photon production in association with additional jets has also been explored [72], however finding than a substantial reduction of the experimental uncertainties, as compared with available measurements, would be mandatory before this data could be used effectively in PDF fits. While LHC photon data has still not been directly included in global PDF fits, a systematic comparison between PDFs and direct photon data was presented by ATLAS [73].

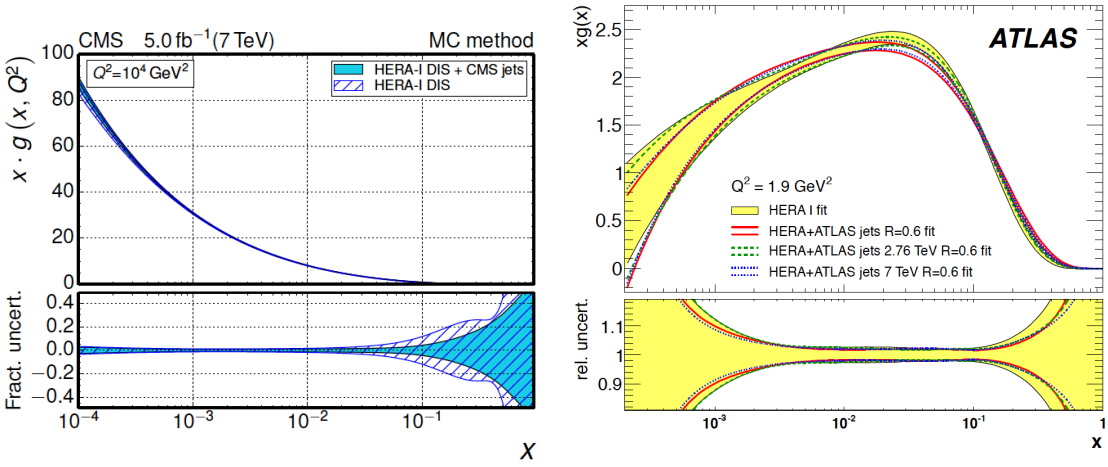

Figure 3: Left plot: impact of the CMS 2011 inclusive jet data on the gluon PDF, from Ref. [41]. Right plot: impact of the ATLAS measurement on the ratio of inclusive jet cross-sections between 7 TeV and 2.76 TeV on the gluon PDF, from Ref.

3.3 Inclusive W and Z production and asymmetries

The inclusive production of W and Z bosons, both for the total cross-sections, the differential measurements in terms of leptonic rapidities and the corresponding asymmetries have been part of the global PDF fit backbone since the first measurements from the Tevatron became available. As compared to inclusive DIS, where only flavor symmetric components $q + \bar{q}$ can be constrained, inclusive W and Z production provides a clean handle on quark flavor separation. At the LHC, the kinematical range in terms of the underlying Bjorken-x is substantially increased as compared to the Tevatron, reaching both smaller and larger values of x. With this motivation of pinning down the PDF quark flavor separation, a number of measurements have been presented by ATLAS, CMS and LHCb, as will be discussed in more detail in Sect. 4. In addition, as shown by ATLAS, if the rapidity distributions of W and Z bosons is measured simultaneously accounting for the correlations [74] then it is possible to provide a handle on the strangeness content of the nucleon [22].

3.4 High and low mass Drell-Yan production

Data from fixed-target Drell-Yan experiments, such as E605 and E866, has been included in global PDF fits since many years. These data however are affected by some drawbacks, in particular the missing covariance matrix and the fact that $\sqrt{s}$ is small and thus perturbative and non-perturbative corrections to fixed order calculations are potentially large. This has provided the motivation to perform for the first time the measurements of the off-peak Drell-Yan processes at an hadron collider. At low mass, Drell-Yan provides interesting constraints on the low-x quarks and gluons (since the latter are radiately generated from the former), as well as tests of perturbative QCD, since breakdown DGLAP [75]. At high-masses, first of all the measurement of Drell-Yan provides a crucial validation of

theory calculations in a region which is instrumental for New Physics searches. Concerning PDFs, high-mass Drell-Yan allows to obtain information from the high-x quarks and anti-quarks, which are affected by substantial uncertainties, particularly for the latter. To maximize the impact of the data in PDF fits, it is essential to use the most updated NNLO QCD and NLO EW theory calculations [76].

In addition, note that low and high-mass Drell-Yan production are sensitive to the photon PDF $\gamma(x, Q^2)$: indeed, since $\gamma\gamma \to l^+l^-$ production is t-channel, as opposed to the s-channel quark-induced diagrams $q\bar{q} \to l^+l^-$, photon-initiated contributions become comparable to quark-initiated at low and high invariant di-lepton masses. Therefore, off-peak Drell-Yan production allows to provide important constraints on the photon PDF [77] for PDF fits which account for QED corrections [78, 79].

3.5 The transverse momentum of W and Z bosons

The transverse momentum of the W and Z bosons is a key process for hadron collider phenomenology. At low p_T, it is used to validate Monte Carlo predictions, analytical resummed calculations, and is a must of many precision measurements like the W mass. At large values of the transverse momentum, we would expect that fixed-order theory to lead to a reasonable description of the data. For large p_T, the transverse momentum distribution of W and Z bosons uniquely depends on the combination $\alpha_s \times q \times g$, where the fraction of gluon-initiated contributions increases with p_T. Therefore, one might want to use the high-p_T spectrum of W and Z bosons as a direct probe of the gluon PDF. This option seems particularly robust for the case of the Z p_T, where a high precision measurements can be performed in terms of leptonic variables only [80]. A complementary use if the W and Z p_T measurements for PDF constraints can be obtained from taking their ratios. As motivated in Ref. [33], various ratios of W and Z cross sections at high p_T provide a handle on the proton's flavor decomposition, while canceling various theoretical uncertainties like higher order QCD and EW effects.

Note also that the LHC has produced a number of measurements of W and Z boson production in association with jets. The main motivation for these measurements is to validate Monte Carlo event generators, but given that the underlying dynamics are the same as those that generate the vector boson p_T, it is conceivable that these can also be used for PDF fits. However, these measurements will be affected by larger theoretical uncertainties (due to the multiplicity of the final state) and experimental uncertainties (due to having jets in addition to leptons) than the W or Z p_T measurement, and thus might not be competitive with the latter.

3.6 W production in association with charm quarks

The production of W bosons in association with charm quarks has been proposed for a long time as a direct probe of the strangeness content of the proton [81]. Indeed, before the LHC stat-up, constrains on strangeness from global fits were provided mostly by low-energy neutrino data, in particular by the dimuon charm production measurements. At the LHC, independent constraints on the strangeness can now be provided by $W + c$ [34], and also the differences between s^+ and s^- can be potentially be investigated with charge ratios such as $W^+ + c/W^- + c$. As we will discuss in the next Section, this measurement has

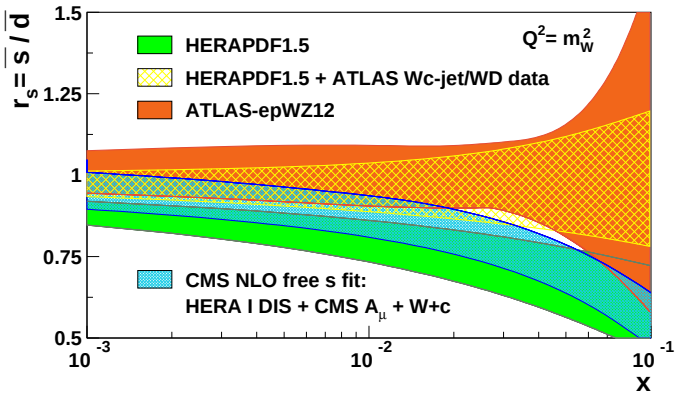

Figure 4: Strange content of the proton quark sea. ATLAS results based on Z and W-boson production measurements [22] and on the associated production of W+charmed hadrons [25] are compared to the CMS result [21], based on the W+c production [24]. For comparison, HERAPDF1.5 is shown, where the constraints on the s-quark distribution as obtained in the neutrino-scattering experiments, are considered.

been presented recently both by ATLAS and CMS, and is already part of some global PDF fits. A topic that has attracted lots of attention recently is whether the LHC $W + c$ data suggest a symmetric strange sea, opposite to neutrino charm data which clearly indicates a strangeness suppression. The ultimate global analysis combining both fixed target and collider data for the strangeness [17, 26]. As an illustration, in Fig. 4 we show the CMS determination of $xs(x, Q^2)$ from their W+charm measurements, from Ref. [21].

3.7 Top quark pair production

Top quarks are abundantly produced at the LHC, where the increase in the center of mass energy and in the luminosity make it a "top factory". As opposed to the Tevatron, where top quark pairs are produced predominantly via quark-anti-quark annihilation, at the LHC top quark pairs are produced mostly in the gluon-gluon channel. Therefore, they potentially provide useful information on the gluons for $x \geq 0.1$, a region which in global fits is only covered by jet production. While NLO calculations are affected by large scale uncertainties, the completion of the full NNLO calculation for total cross-sections [82] and for differential distributions [83] allows to consistently include top quark data in global PDF fits. In the latter case, it is also possible to use approximate NNLO calculations derived from threshold resummation [28]. Note that the availability of NNLO calculations allows to perform a number of complementary extractions of fundamental QCD parameters, like α_s, from total cross-sections [84].

With this motivation, a number of studies have quantified the sensitivity of top quark pair production data to the gluon PDFs. Using total cross-sections, it has been shown that available data from ATLAS and CMS is enough to produce useful constrains on the large-x gluon [27, 36]. The ABM collaboration has also explored the impact of top quark cross-sections into their fit, showing that it can lead to a shift in the gluon PDF

up to one-sigma [13]. However, the usefulness of total cross-sections is only moderate, and the full constraining power of top quark data for PDF fits should be based on the differential distributions. A first study on this respect, based on the approximate NNLO from threshold resummed calculation, has been presented in Ref. [28].

3.8 Charm and bottom pair production

The production of heavy quark pairs in hadron collisions is a powerful test of perturbative QCD. While as mentioned in the previous section top quark pair production is now usually included in PDF fits, this is not the case of charm and bottom pair production. On the other hand, the differential distributions in p_T and rapidity of charm and bottom quarks are directly sensitive to the small-x gluon PDF at low scales, where its uncertainties are large, and thus this measurement is potentially a useful probe of the small-x gluon. In this respect, measurements of the $d^2\sigma/dp_T dy$ differential distributions of charm and bottom mesons at the LHC should provide a direct information on the poorly known gluon PDF.

These constraints are expected to be particularly powerful from the LHCb experiment, since on the one hand the detector is specially suitable to tag and measure with precision the properties of heavy quark mesons, and on the other hand the forward coverage of LHCb allows to access a region of small-x of the gluon PDF that cannot be accessed by ATLAS and CMS. The first study [29] in this direction is performed by the PROSA Collaboration, where the impact of recent measurements of heavy-flavor production at LHCb is studied in a QCD analysis at NLO in fixed-flavor number scheme using the HERAFITTER framework. Significant improvement of constraints on the gluon and the sea-quark distributions down to $x \sim 5\,10^6$ is demonstrated, as illustrated in Fig. 5. A major problem is though that the usefulness of this data for PDF fits is limited by the large theory uncertainties in the NLO calculation, however it is conceivable that the recent NNLO calculation for differential distributions in top-quark production [83] can also be generalized to bottom and charm production.

3.9 Central exclusive production

As has been mentioned on Sect. 3.8, the production of charm and bottom quarks at the LHC provides useful constraints on the low-x gluon. A related processes, which can potentially provide the same information, is central exclusive production of J/ψ and related mesons, such as Γ or $\psi(2S)$ The production of these mesons depends directly on the small-x gluon. In addition, the production mechanism is such that a very clean final state is obtained. Calculations for the central exclusive production have been presented in Refs. [85, 86] within the diffractive photo-production formalism. In order to consistently incorporate this processes into traditional PDF fits, it should be possible to related available calculations with the collinear factorization picture, which is used in global PDF fits.

3.10 Ratios of cross-sections for different center-of-mass energies

The staged beam energy of the LHC running, with data available at a number of different center of mass energies, allows to construct a novel type of observables, namely ratios and double ratios of cross-sections measured at different center of mass energies [37]. The

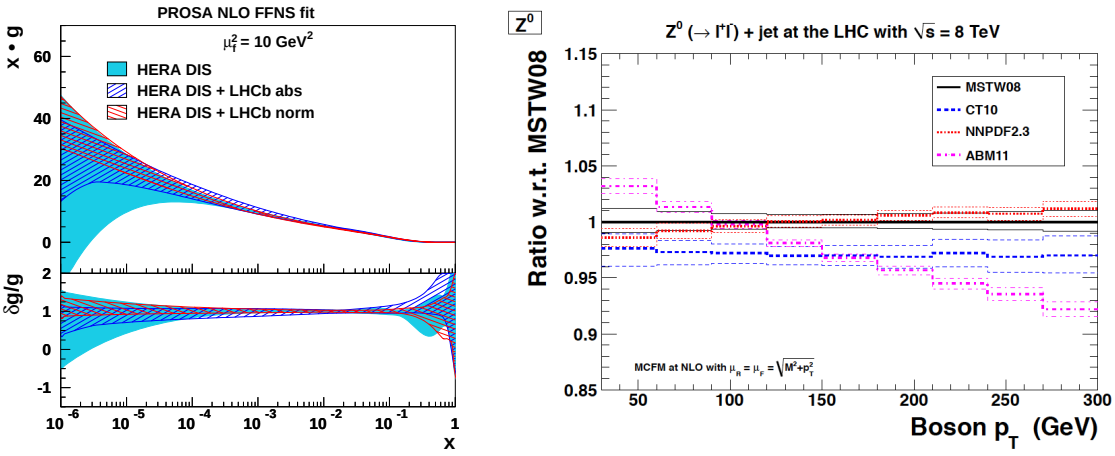

Figure 5: Left plot: gluon distribution (top) and its relative uncertainty (bottom), shown as a function of x at the factorization scale of 10 GeV^2. Results of the NLO QCD analysis [29]. of HERA-I DIS data only (filled band) and of that including either absolute or normalized cross sections of heavy-flavor production at LHCb (dashed bands) are compared. Right plot: Z pt ...

main advantage of this construction is that, by taking the ratio, a number of experimental and theoretical systematics will approximately cancel. This way, we end up with an observable that can be predicted with very high accuracy (because of the cancellation of some important theory systematics, like higher orders), and that can potentially be measured with high precision as well, due to the cancellations of systematic uncertainties such as jet energy scale or luminosities. From the PDF point of view, the interest in these ratios is that precisely part of the PDF dependence does not cancel, because data at different $\sqrt{s}$ will cover a different range in x and Q^2, and therefore we can think of including these ratio data to constrain PDFs. Another advantage is that the constraints from the ratios can be complementary to those of the absolute cross-sections: for example, in top quark production, the dependence on the value of m_t will completely cancel in this ratio.

From the experimental point of view, the crucial point is to quantify the degree of correlation of different systematics between different values of $\sqrt{s}$. Up to know, there have been two measurements that have implemented this idea: the ratio of inclusive jet cross-sections between 7 TeV and 2.76 TeV from ATLAS [19] and the ratio of Drell-Yan cross-sections between 7 and 8 TeV at CMS [38]. While these two measurements are very important as proof-of-concept, they impact on PDF fits will be moderate due to the reduced statistics of the 2.76 TeV sample (for ATLAS) and the small lever arm between 7 and 8 TeV (for CMS). However, now at Run II a number of ratios between 13 TeV and 8 TeV should be measurement, and this could become part of the fitted dataset in global analysis.

ATLAS				
Measurement	$\sqrt{s}$, year of data, $\mathcal{L}_{\rm int}$	Motivation	Reference	PDF fits
W, Z rapidity	7 TeV, 2010, 36 pb^{-1}	Sect. 3.3	[74]	[13, 16, 17, 22, 60]
High mass Drell-Yan	7 TeV, 2011, 4.9 fb^{-1}	Sect. 3.4	[32]	[16, 17, 78]
Low mass Drell-Yan	7 TeV, 2010, 35 pb^{-1}	Sect. 3.4	[87]	-
	7 TeV, 2011, 1.6 fb^{-1}			
Z A_{FB}	7 TeV, 2011, 4.8 fb^{-1}	Sect. 3.4	[88]	-
W+charm production	7 TeV, 2011, 4.6 fb^{-1}	Sect. 3.6	[25]	[25]
W+beauty production	7 TeV, 2010, 35 pb^{-1}	Sect. 3.6	[89]	-
W+beauty production	7 TeV, 2011, 4.6 fb^{-1}	Sect. 3.6	[90]	-
Z+beauty production	7 TeV, 2010, 36 pb^{-1}	Sect. 3.6	[91]	-
Z+beauty production	7 TeV, 2011, 4.6 fb^{-1}	Sect. 3.6	[92]	-
Z p_T	7 TeV, 2010, 40 pb^{-1}	Sect. 3.5	[93]	
Z p_T	7 TeV, 2011, 4.7 fb^{-1}	Sect. 3.5	[80]	
W p_T	7 TeV, 2010, 31 pb^{-1}	Sect. 3.5	[94]	[17]
Z+jets	7 TeV, 2010, 36 pb^{-1}	Sect. 3.5	[95]	-
Z+jets	7 TeV, 2011, 4.6 fb^{-1}	Sect. 3.5	[96]	-
W+jets	7 TeV, 2010, 36 pb^{-1}	Sect. 3.5	[97]	-
W+jets	7 TeV, 2011, 4.6 fb^{-1}	Sect. 3.5	[98]	-
$R_{\rm jets}$ (W+jets/Z+jets)	7 TeV, 2011, 4.6 fb^{-1}	Sect. 3.5	[99]	-

Table 2: Overview of published PDF-sensitive measurements from the LHC Run I from the ATLAS experiment. In this table, for each of the measurements, we provide first of all the corresponding center-of-mass energy, year of data, and the integrated luminosity, its motivation in terms of PDF sensitivity, the publication reference and the references where these measurements have been used to quantify PDF constraints.

4 Constraining PDFs with LHC data at Run I

In this section we present a concise overview of those LHC measurements at Run I with potential sensitivity to PDFs. The motivation for each of these measurements has already been discussed in Sect. 3, so now we discuss the specific analysis that have been performed at the LHC and, where relevant, when these measurements have been used for PDF constraints. This section is organized separately by experiment: we begin with the summary of the results from ATLAS, then CMS and finally with LHCb. For each experiments summary tables are provided. They includes only published or at least submitted to a journal measurements, while superseeded ones are ignored even if they was published. For each measurement shown in the table we provide: the center-of-mass energy at which the measurement was made; the corresponding integrated luminosity; the publication reference and the references where these measurements have been used to quantify PDF constraints. For the CMS table additionnal information if provided if the observable was used in a dedicated extraction of the strong coupling constant and its running.

4.1 Constraints from ATLAS

The measurement from the ATLAS collaboration are summarise in Tables 2 and 3.

We start with the measurements of jet production from ATLAS. The available measurements, relevant for PDF studies, are the inclusive and dijet differential cross sections from the 2010 dataset [100], the ratio of 2.76-to-7 TeV inclusive jet cross sections [19] and, more recently, the inclusive [101], dijet [102] and trijet [103] differential cross sections from

ATLAS				
Measurement	$\sqrt{s}$, year of data, $\mathcal{L}_{\text{int}}$	Motivation	Reference	PDF fits
Inclusive jets	7 TeV, 2010, 37 pb^{-1}	Sect. 3.1	[100]	[16, 17, 60]
Inclusive jets	7 TeV, 2011, 4.5 fb^{-1}	Sect. 3.1	[101]	-
Inclusive jets (+ 7 TeV rat)	2.76 TeV, 2010, 0.2 pb^{-1}	Sect. 3.1, 3.10	[19]	[16, 17, 19]
Dijets	7 TeV, 2010, 37 pb^{-1}	Sect. 3.1	[100]	-
Dijets	7 TeV, 2011, 4.6 fb^{-1}	Sect. 3.1	[102]	-
Trijets	7 TeV, 2011, 4.5 fb^{-1}	Sect. 3.1	[103]	-
γ inclusive production	7 TeV, 2010, 35 pb^{-1}	Sect. 3.2	[104]	-
γ inclusive production	7 TeV, 2011, 4.6 fb^{-1}	Sect. 3.2	[105]	[73]
γ+jets	7 TeV, 2010, 37 pb^{-1}	Sect. 3.2	[106]	-
$t\bar{t}$ incl (single lepton, dilepton)	7 TeV, 2010, 2.9 pb^{-1}	Sect. 3.7	[107]	[16]
$t\bar{t}$ incl (dilepton)	7 TeV, 2010, 35 pb^{-1}	Sect. 3.7	[108]	[16]
$t\bar{t}$ incl (single lepton)	7 TeV, 2010, 35 pb^{-1}	Sect. 3.7	[109]	[16]
$t\bar{t}$ incl (dilepton)	7 TeV, 2011, 0.70 fb^{-1}	Sect. 3.7	[110]	[16, 17]
$t\bar{t}$ incl (e/μ + τ)	7 TeV, 2011, 2.05 fb^{-1}	Sect. 3.7	[111]	[16]
$t\bar{t}$ incl (tau+jets)	7 TeV, 2011, 1.67 fb^{-1}	Sect. 3.7	[112]	[16]
$t\bar{t}$ incl (eμ b-tag jets)	7+8 TeV, 2012, 24.9 fb^{-1}	Sect. 3.7	[113]	[17]
$t\bar{t}$ differential	7 TeV, 2011, 2.05 fb^{-1}	Sect. 3.7	[114]	-
$t\bar{t}$ differential	7 TeV, 2011, 4.6 fb^{-1}	Sect. 3.7	[115]	-
WW, $Z \to \tau\tau$, $t\bar{t}$ xsec	7 TeV, 2011, 4.6 fb^{-1}	Sect. 3.3	[116]	-

Table 3: Continuation of Table 2.

the 2011 dataset. In ATLAS own analysis [19], a PDF fit of the ratio of 2.76 TeV over 7 TeV inclusive jet data (together with HERA data) was performed, to demonstrate the sensitivity to the large-x gluon PDF, by comparing to a baseline fit based on HERA data only. Though the measurement has limited statistics, it is a powerful proof-of-principle that such ratio measurements have enhanced PDF sensitivity due to the partial cancellation of dominant theoretical (missing high order corrections) and experimental (jet energy scale) systematic uncertainties, as discussed in Ref. [37].

The more recent measurements of inclusive, dijet and trijet differential cross sections have substantially higher precision compared to previous measurements, and span a wide kinematic range, extending up to 2 TeV in inclusive jet p_T, and up to 5 TeV in dijet or trijet invariant mass. The inclusive and dijet ATLAS analyses include quantitative χ^2 comparisons for the predictions of different PDF sets, showing clear discriminating power. Furthermore, these inclusive, dijet and trijet measurements from the 2011 dataset are particularly interesting for PDF fits since, for the first time, the full statistical and systematic correlations between various measurements will be provided, allowing their simultaneous inclusion in a PDF fit, and thus enhancing its PDF constraining information. The jets are reconstructed using the anti-k$_T$ clustering algorithm [117], and the cross section measurements are available separately for two radius parameters: R=0.4 and R=0.6.

At the LHC, top quark pair production is sensitive to the gluon PDF, providing information complementary to jet production data. The ATLAS Collaboration have made a number of measurements of top quark pair production, including several extractions of the top quark pair production cross section [107–113] with increasing precision and using a variety of final states, are well as differential cross sections using the 2011 [114, 115] dataset. In the most recent of these measurements, using the full 2011 dataset, the normalized differential cross sections are measured as a function of the top quark transverse momen-

tum, and of the mass, transverse momentum and rapidity of the top quark pair system. Normalizing the cross sections reduces the dependence on higher order QCD corrections, though it also degrades a bit the sensitivity to the gluon PDF overall normalization. When compared to a range of PDFs, the measured data distributions tend to be softer than the predictions, indicating power to constrain the gluon, and may also indicate the importance of higher order QCD and electroweak corrections.

Isolated prompt photon data also have the potential to provide additional constraints on the gluon at medium and large-x. Compared to jet production, prompt photons provide a cleaner experimental environment, though current measurements are of limited precision. ATLAS have measured isolated prompt photon production cross sections in the 2010 [104] and 2011 [105] datasets. The most recent measurement, using the 2011 data, provides differential cross section as a function of photon transverse energy and pseudo-rapidity, in central and forward pseudo-rapidity regions. The ATLAS Collaboration have studied [73] the sensitivity of these 2011 data to PDFs, providing a quantitative χ^2 comparison of the agreement of data with NLO QCD predictions for a range of PDFs. The results indicate some tension between data and theory for several current PDFs, indicating potential to constrain the shape and uncertainty of the gluon, though theoretical scale uncertainties are also large. Measurements of prompt photons in association with jets [106] are also available.

Electroweak boson production data provide constraints on quark flavor separation. ATLAS have published W and Z rapidity distributions using the 2010 data, including their experimental correlations [74]. This measurement is now part of most, current PDF fits. In a separate ATLAS analysis, these data were used in a PDF fit with the `HERAfitter` framework to quantify the sensitivity to the strange quark content of the proton [74], and favored a non-suppressed strangeness. The ATLAS inclusive W and Z analysis of 2011 data is also close to publication. The larger dataset allows more differential measurements, for example double differential Z/γ^* cross sections binned in dilepton mass and rapidity, and $W^{\pm}$ cross sections in bins of lepton pseudo-rapidity, as well as double differentially in lepton pseudo-rapidity and lepton transverse momentum. These data have the potential to provide constraints on valence quark PDFs, and will shed further light on the strangeness content of the proton.

ATLAS has also published high [32] and low [87] mass Drell Yan measurements, providing complementary information to measurements near the Z mass peak. The ATLAS low mass Drell-Yan cross sections are measured as a function of dilepton invariant mass with coverage $26 < mll < 66$ GeV (partial 2011 dataset) and $12 < M_{ll} < 26$ GeV (for the 2010 dataset). High-mass Drell Yan measurements can provide important constraints on large x quarks and anti-quarks. The ATLAS analysis, based on the 2011 dataset, measure up to 1.5 TeV in dilepton invariant mass, and the data have been included in recent PDF fits [16, 17]. In addition, in the prensence of QCD corrections, this measurement can also be used to constraint the photon content of the proton, and have been included in the NNPDF2.3QED fit [78]. A higher precision measurement at 8 TeV is also being prepared.

ATLAS have also provided a measurement of W+charm data, using the 2011 dataset [25]. Such data give a direct handle on the strange content of the proton, and the ratio of $W^+\mathrm{c}$ to $W^-\mathrm{c}$ is also sensitive to the strange asymmetry, $s - \bar{s}$. The ATLAS analysis has shown the data are consistent with a range of PDFs, though indicate a preference for PDFs with an $SU(3)$ symmetric light quark sea, consistent with the result found by the ATLAS

CMS				
Measurement	$\sqrt{s}$, $\mathcal{L}_{\rm int}$	Motivation	Reference	Used in PDF or α_s fits
High and low mass Drell-Yan	7 TeV, 5 fb^{-1}	Sect. 3.4	[31]	[16, 69]
High and low mass Drell-Yan	8 TeV, 20 fb^{-1}	Sect. 3.4	[38]	
Drell-Yan AFB	7 TeV, 5 fb^{-1}	Sect. 3.4	[119]	–
W asymmetry	7 TeV, 36 pb^{-1}	Sect. 3.3	[120]	
W e asymmetry	7 TeV, 880 pb^{-1}	Sect. 3.3	[121]	
W μ asymmetry	7 TeV, 4.7 fb^{-1}	Sect. 3.3	[21]	[21, 69]
W, Z production and rapidity dist	7 TeV, 3 pb^{-1}	Sect. 3.3	[122]	
W, Z inclusive production	7 TeV, 36 pb^{-1}	Sect. 3.3	[123]	–
W, Z inclusive production	8 TeV, 19 pb^{-1}	Sect. 3.3	[124]	–
Z p_T and rapidity	7 TeV, 36 pb^{-1}	Sect. 3.5/3.3	[125]	
Z p_T and rapidity	7 TeV, 5 fb^{-1}	Sect. 3.5/3.3	add ref	
Inclusive jets	7 TeV, 5 fb^{-1}	Sect. 3.1	[20] and [126]	[16, 41, 60]
Dijets	7 TeV, 5 fb^{-1}	Sect. 3.1	[20]	–
Three-jets	7 TeV, 5 fb^{-1}	Sect. 3.1	[127]	[127]
Three-jets/Di-jets ratio	7 TeV, 5 fb^{-1}	Sect. 3.1	[42]	[42]
W+charm	7 TeV, 5 fb^{-1}	Sect. 3.6	[24]	[21, 26, 60]
Z+beauty	7 TeV, 5 fb^{-1}	Sect. 3.6	[128]	–
γ inclusive production	7 TeV, 36 pb^{-1}	Sect. 3.2	[129]	[23]
γ+jets	7 TeV, 2.1 fb^{-1}	Sect. 3.2	[130]	–
$t\bar{t}$ inclusive	7 TeV, 2.3 fb^{-1}	Sect. 3.7	[131]	[27, 28, 84]
$t\bar{t}$ differential	7 TeV, 5.0 fb^{-1}	Sect. 3.7	[132]	[28]
$t\bar{t}$ inclusive	8 TeV, 1.14 fb^{-1}	Sect. 3.7	[133]	[27]
$t\bar{t}$ inclusive	8 TeV, 2.8 fb^{-1}	Sect. 3.7	[134]	[27]
$t\bar{t}$ inclusive	8 TeV, 2.4 fb^{-1}	Sect. 3.7	[135]	[28]

Table 4: Same as Table 2, for the CMS experiment. In the last column, we also indicate which of these measurements have been used as input for a determination of the strong coupling α_s.

analysis of the 2010 W and Z rapidity distributions. Measurements of vector boson in association with beauty are also available [89–92], though these are more useful to test of pQCD calculational schemes, like $N_f = 4$ versus $N_f = 5$ [118], than for PDF studies.

Vector boson production in association with jets provide further sensitivity to the gluon and sea quark PDFs. ATLAS have made a number of measurements of W+jets and Z+jets using 2010 or 2011 data [95–98]. In addition, ATLAS have measured the W+jets/Z+jets ratio [99], which is complementary to the individual W+jets and Z+jets measurements, and is especially interesting due to the large cancellation of experimental systematic uncertainties and non-perturbative QCD effects.

Vector boson transverse momentum distributions are also sensitive to the gluon and quark PDFs over a wide range of x. ATLAS have measured the W p_T [94] distribution with 2010 data, and the Z p_T distribution with 2010 [93] and 2011 [80] data.

4.2 Constraints from CMS

The measurement from the CMS collaboration are summarise in Table 4.

High-precision measurements of the cross-sections of multi-jet production in proton-proton collisions have been performed by the CMS collaboration and the systematic correlations were investigated. The potential of several CMS jet measurements to constrain the PDFs and determine the strong coupling was demonstrated by the CMS collaboration.

In the following the details of the relevant measurements are provided. The measurement of inclusive jet production cross-sections in pp collisions at $\sqrt{s}$=7 TeV as a function of jet kinematics based on the data collected in 2011 is published in Ref. [20]. Jets are reconstructed with the same algorithm than in ATLAS but a different value of radius parameter, R = 0.7.

One shall notice that this choice is common for all jet analyses performed with only jets in the final state. This choice was motivated by the fact that a smaller cone is more sensitive to the final state radiation effects that are not well described by the NLO predictions in QCD. A dedicated analysis was designed to test this statement by considerint the inclusive jets cross section ratio measured using the same data but two different radii parameters: 0.5 and 0.7 [126]. In this paper an inclusive jets cross section with R=0.5 is also presented, as well as the cross section with R=0.7 extrapolated toward a lower p_T. In contrary when an associated production of jets with vector bosons are considered traditionally R=0.5 choice is preferred.

A comprehensive QCD analysis [41] of this measurement was performed by the CMS collaboration to demonstrate the impact of these data on the PDFs and to determine the strong coupling constant. Furthermore, the correlations of the systematic uncertainties were reanalyzed and the recommendations for usage of the measurement [20] in the PDF fits were published [41]. The impact of the inclusive jet measurement on the PDFs of the proton is investigated in detail using the `HERAfitter` tool [43], using both the Hessian [136] and the Monte Carlo methods [71].

When the CMS inclusive jet data are used together with the HERA-I DIS measurements, the uncertainty in the gluon distribution shrinks all over the phase-space. In particular a significant reduction is observed for the parametric uncertainty. At the same time, a modest is induced in uncertainties on the knowledge of u and d valence quark distributions, consistent with the dominance of qq scattering of jet production at high p_T. The inclusion of the CMS inclusive jet data also allows a combined fit of $\alpha_S(M_Z)$ and of the PDFs, which is not possible with the HERA-I inclusive DIS data alone. As summarized in Table 4, these inclusive jets results are already used by several PDF collaborations. The still ongoing inclusive jets measurements at CMS are expected to extend and complement the Run I legacy picture at different center-of-masses.

Two measurements of the three-jet cross section have been performed and optimized for the extraction of α_S running. The first one [42] used the ratio between the three jets cross section and the dijet cross section that is at leading order proportional to α_S. This observable has a reduced dependence to the proton PDF and instrumental to partially decouple the measurement of α_S from the gluon density in the proton. The second analysis [127] makes usage of the three jet mass spectrum and is proportional at the leading order to α_S^3. This observable is more sensitive than the previous one, but is also more dependant to the choice of the proton PDF and suffers from larger systematics.

The three measurements together provide for the first time a stringent test of the strong coupling running in the region between 100 GeV and 2 TeV. In particular, these are the first direct measurements of the strong coupling constant in the TeV scale, that can be used to provide constraints on BSM scenarios [137].

Using the data collected with CMS detector in 2011 at $\sqrt{s}$=7 TeV, also the dijet cross-sections [20] have been measured. One should notice that the dijet measurement exhibits a significant statistical correlation with the inclusive jets measurement. Since no

statistical correlation matrix was provided between the various CMS jet measurements, it is not possible to use them at the same time in a PDF analysis.

A significant effort within the CMS collaboration has been devoted to the precise measurements of the inclusive vector boson production. We can identify three sets of measurements: the neutral and charged Drell-Yan (DY) production with a particular attention dedicated to the Z peak; the charged lepton radial asymmetry in the W production (hereafter referred as W asymmetry); the high p_T bosons production. The first two sets of measurements are expected to be mainly sensitive to quark density, while the third one to the gluon density.

The inclusive measurements in electrons and muons channel of the on-peak neutral and charged DY cross section were performed at 7 and 8 TeV using the first low luminosity data with a in order to reduce the contamination from the pile-up [122–124]. Subsequently a precise double-differential cross section in lepton pairs mass and rapidity was performed normalized to the peak cross section [31,38]. A full correlation matrix between bins of the normalized measurement as well as the peak cross section is provided. Moreover the 8 TeV analysis was designed in such a way to make easy the ratio measurement of 8 over 7 TeV cross sections. This extremely precise result with typical uncertainties at the percentage level in the bulk of the cross section is ready to be used by PDF extraction groups and its real sensitivity to the parton densities still needs to be assessed.

The tensor properties of the DY events was further studied using the forward-backward asymmetry in DY events [119] and subsequently used to extract the effective Weinberg angle [138]. It may also provide a certain sensitivity to the PDFs that was not yet studied.

The lepton charge asymmetry measurements in W-boson production were performed separately with muons and electrons that are sensitives to different experimental systematic effects. The most precise measurement available today [21] remains the muon charge asymmetry measurement at CMS, performed with the full 7 TeV data set, while the electron charge asymmetry is limited by the available p_T single lepton trigger to 880 pb^{-1} data sample [121]. The sensitivity of the muon charge asymmetry to the valence quark density was studied in a QCD analysis at NLO in [21]. A significant reduction of the uncertainty on the d-valence and u-valence distributions with respect to a PDF fit in which only HERA I inclusive DIS data are used. The lepton charge asymmetry is now a standard component of the PDF extraction by many specialized groups. Even more precise measurement of muon charge asymmetry at $\sqrt{s} = 8$ TeV by the CMS collaboration is ongoing.

Finally the on-peak Z boson measurement double differentially in p_T and y was designed and performed (add ref) to provide a tool to extract the gluon density with a percentage level experimental precision in the muon channel. The available prediction for the boson production with $p_{\mathrm{T,Z}} \approx M_{\mathrm{Z}}$ are only NLO in α_s, while an NNLO prediction seems to be necessary to take the full advantage of this precision.

CMS carried out an important program of measurements for vector boson production associated to the heavy flavors. Cross sections of the associated production of the W-boson together with charm quark is measured differentially in charged lepton rapidity at 7 TeV [24]. This measurement provides a direct probe of the strange-quark content of the proton sea, as demonstrated by the CMS collaboration in a QCD analysis [21] at NLO, in which HERA-I DIS data, measurements of muon charge asymmetry and the cross sections of W+c productions are used. Strange-quark content, determined in the analysis [21] is demonstrated to be consistent with results of the neutrino-scattering experiments. The

$Z+b$ production at 7 TeV is measured single-differentially due to a lack of statistics, but a differential measurement is expected to be provided at 8 TeV. The measurements of gauge boson production in association with heavy quarks provide useful information on pQCD calculational techniques, in particular massive versus massless calculations.

Top-quark pairs in proton-proton collisions are produced predominantly through gluon-gluon fusion. Measurements of the top-pair production at the LHC probe the gluon distribution at high x and at the same time provide constraints on the top-quark mass and the strong coupling constant. For the first time, the value of α_s was determined [84] at NNLO using the inclusive $t\bar{t}$ production cross section measured by the CMS collaboration [131]. The impact of the inclusive cross section of $t\bar{t}$ production on the gluon distribution is studied [27], where the CMS measurements at $\sqrt{s} = 7$ TeV [131] and $\sqrt{s} = 8$ TeV [133, 134] are included.

In the QCD analysis [28], the inclusive and differential cross sections of the top-quark pair production are included and a moderate reduction of the uncertainty on the gluon distribution at high x is demonstrated. In this analysis, the CMS measurements of total [131, 135] and differential [132] top-pair production cross sections are used. More significant improvement of the precision of the gluon distribution is expected with more precise data of the LHC at higher energies. It is important to notice, that for future PDF fits using the top-pair production measurements, the parton-level cross sections in the full phase space should be provided supplemented by the information about correlations of the statistic and systematic uncertainties, also between the data sets of different energies and between (normalized) differential and inclusive cross section measurements.

4.3 Constraints from LHCb

The LHCb experiment, thanks to its unique forward coverage, extends the kinematical range covered by ATLAS and CMS and in particular allows to explore in better detail the small-x region [139]. Therefore, even for the same underlying physical process, LHCb measurements are fully complementary to those of ATLAS and CMS. The corresponding overview of LHCb results are summarized in Table 5. We now discuss the results in some detail.

Measurements of W and Z production using muon final states have been performed with 37 pb^{-1} of data collected in 2010 [140]. These measurements, along with those of Z production in the di-electron channel at 7 TeV [141], have been incorporated by the NNPDF collaboration into their PDF fit [17]. The W cross-section and lepton asymmetry measurements have since been updated with the full 2011 dataset [142]. The precision is significantly improved due to the larger data sample, a better understanding of the detector effects, and an improved luminosity determination [143]. An updated measurement of Z production at 7 TeV in the muon channel is expected to be published in 2015 and will benefit from a similar improvement in precision. As regards the dataset collected in 2012 at a centre-of-mass energy of 8 TeV, Z production has been measured in the di-electron channel [144], with W and Z measurements in the more precise muon channels expected to follow in 2015.

Low-mass Drell-Yan measurements at LHCb are sensitive to x values as low as 8×10^{-6} at $Q^2 = 25$ GeV^2. A preliminary measurement has been performed by the collaboration at 7 TeV [145] and work is ongoing to finalize the result with the Run-I dataset. Mea-

LHCb				
Measurement	$\sqrt{s}$, $\mathcal{L}_{\rm int}$	Motivation	Reference	Used in PDF fits
W, Z muon rap dist	7 TeV, 37 pb^{-1}	Sect. 3.3	[140]	[17]
W muon rap dist	7 TeV, 1.0 fb^{-1}	Sect. 3.3	[142]	
$Z \to ee$ rap dist	7 TeV, 0.94 fb^{-1}	Sect. 3.3	[141]	[17]
$Z \to ee$ rap dist	8 TeV, 2.0 fb^{-1}	Sect. 3.3	[144]	
$c\bar{c}$ production	7 TeV, 15 nb^{-1}	Sect. 3.8	[30]	-
$b\bar{b}$ production	7 TeV, 0.36 fb^{-1}	Sect. 3.8	[148]	-
Exclusive J/ψ production	7 TeV, 1.0 fb^{-1}	Sect. 3.9	[149]	-

Table 5: Same as Table 2, for the LHCb experiment.

surements have also been performed of Z production in association with b-quarks and D mesons [146, 147] and there is also ongoing progress with Run I data to measure the cross-sections for top quark production and W production in association with beauty and charm jets at LHCb.

Measurements of inclusive beauty and charm quark production have been performed [30,148] using data collected in 2010 and 2011 at 7 TeV. The measurements exploit LHCb's particle identification and vertexing capabilities to fully reconstruct B and D mesons using hadronic decay modes. As discussed in Sect. 3.8, heavy flavor production can be used to constrain the gluon distribution at low-x and the impact of these results on the PDFs is under study by a number of groups.

As discussed in Sect. 3.9, precise measurements of J/ψ and Υ photo-production can also lead to strong constraints on the low-x gluon distribution [85]. As these processes are characterized by events containing just two muon tracks and a large rapidity gap, LHCb is well suited to their detection due to its relatively low pile-up running conditions and partial backward coverage. Measurements have been made of central exclusive J/ψ production at a centre-of-mass energy of 7 TeV [149] with measurements of Υ production expected in 2015.

5 Prospects for Run II measurements

In the last part of this document, we now turn to discuss the plans from ATLAS, CMS and LHCb concerning PDF-sensitive measurements from Run II. Of course some of the discussion here will be speculative, but it is useful to have a general overview of which PDF measurements will be done in the short, the medium and the long term from the LHC. Let us also mention that in the near future information relevant for PDFs will also be provided by other experiments, including HERA, JLab and SeaQuest among others, but here we restrict ourselves to the prospects at the LHC As in the previous section, we proceed sequentially, first of all with the ATLAS plans, then the CMS plans and finally the LHCb plans.

5.1 Prospects from ATLAS

The ATLAS Collaboration will continue to make measurements sensitive to PDFs in Run II. The higher center-of-mass energy corresponds to larger cross sections and extended kinematic reach for many processes of interest, and the increase in integrated luminosity should lead to a significant reduction of statistical and systematic uncertainties.

For inclusive electroweak vector boson production, the cross section increases by a factor of 1.7 (1.9) for 13 TeV compared to 7 (8) TeV, and probes a different x regime, providing complementary PDF sensitivity. In addition to measurements of the total and fiducial cross sections of inclusive W and Z production with extended coverage, of particular interest are cross section ratios (W^+/W^- and W/Z), which benefit from the partial cancellation of many systematics. Furthermore, measurements at Run II will complement those already made (or soon to come) from LHC Run I at 7 and 8 TeV. In order to maximally benefit from the LHC data at both Run I and II, a careful consideration of the experimental systematic correlations is necessary from the start. ATLAS will also be able to measure cross section ratio measurements at different center-of-mass energies, and also double ratios of different processes (e.g. $t\bar{t}$, Z, W^+, W^-) at different center-of-mass energies, which are potentially sensitive probes of PDFs, due to the reduction or cancellation of theoretical and experimental systematic uncertainties.

Concerning high mass Drell Yan measurements, at Run II ATLAS will significantly benefit from the higher energy, substantially improving the statistical precision at high dilepton masses of the current measurement, and allowing extended coverage up to 3 TeV, thus providing direct constraints on the poorly known quarks and antiquark PDFs at larger x. Such data can also provide further constraints on the photon PDF. For low mass Drell-Yan production, the Run II data can also potentially improve the experimental precision in the low mass bins of the dilepton invariant mass distribution, providing information down to $x \sim 10^{-4}$, a region where PDF uncertainties are large.

Further ATLAS measurements of vector boson p_T distributions, and of vector bosons in association with jets (including their ratios) are also of interest at 13 TeV, where both the kinematic reach in p_T and the experimental uncertainties can be improved as compared to the corresponding 8 TeV measurements. Ratio measurements of different processes and/or at different center-of-mass energies can enhance PDF sensitivity, but will require careful treatment of correlations.

Measurements of vector boson in association with heavy flavor production are also of

significant interest for PDF studies. So far in Run I, the ATLAS $W + c/W + D^*$ measurements are statistically limited. Run II data can substantially reduce the statistical uncertainty, by up to a factor of 2 with the 2015 data, and potentially allow a widening of phase space (with the extended coverage at low track p_T, provided by the newly inserted Insertable B-layer, IBL). Given that the ATLAS inclusive W and Z in Run I have suggested an enhanced strangeness content of the proton, supported by the current ATLAS Run I W+c data, it is important to measure this process at Run II with the highest precision possible, to shed further light. ATLAS will also be able to make higher precision measurements of vector bosons in association with bottom quarks, providing a means to explore different heavy flavor schemes, among other things.

ATLAS jet measurements at Run II will allow an extended kinematic reach up to inclusive jet transverse momenta of around 3.5 TeV. Again, ratio measurements at different center-of-mass energy, which will require careful consideration of correlated systematics between Run I and Run II data, can give a better control of dominant systematic uncertainties, as already demonstrated by the previous ATLAS measurement of the ratio of the 2.76 to 7 TeV inclusive jet cross sections (see Sect. 4.1). As for Run I, ATLAS measurements of dijet, trijet and multi-jet cross sections will also be possible, extending to higher scales and potentially providing further constraints on PDFs and α_s.

Prompt photon production will also benefit from Run II, providing improved precision on the measurements, which is required for these data to have significant PDF-constraining power. At 13 TeV, the top quark pair production cross section is increased by a factor of 4.7 (3.3) compared to 7 (8) TeV. ATLAS will be able to perform higher precision measurements of total and differential (normalized and absolute) cross sections, as well as ratio measurements at different centre of mass energies, which can help constrain and disentangle the high x gluon PDF, and α_s.

5.2 Prospects from CMS

The prospects for Run II data taking period from the CMS collaboration are rather similar to that of the ATLAS one. There is a rather consensual need to repeat all the basic measurements designed to constraint the proton PDFs at 13 TeV: jets production, DY production, prompt photon and $V + c/V + b$ production. In particular the measurements at 13 TeV are designed in such a way that ratios of cross sections at different center-of-mass energies could be measured with an optimal cancellation of systematic uncertainties. In the following we would highlight few aspects of Run II program specific to the CMS collaboration.

The philosophy behind the precision measurements program at CMS for the Run II is based on the optimal usage of data collected with different running conditions. The LHC collision program forsees few different phases in luminosity ramping:

- A period of data taking with limited PU (typically below 5). Those data if their amount exceeds typically 30 pb^1, would be used for a precise and quick determination of the Z and W boson total production cross section. In particular a limited amount of PU simplifies significantly the extraction of the W cross section and the usage of the electron channel. If the amount of data is large enough a p_T and y spectrum can also be extracted.

- A period of data taking with bunch spacing of 50 ns and with up to 1 fb^{-1} to be collected. Those data benefit from conditions very similar to those at the end of Run I and represents a perfect candidate for a center-of-mass ratio.
- Most of the data would be collected with a bunch spacing of 25 ns. Those data would serve to increase the statistics in high p_T tails and perform the bulk of measurements statistically limited at 8 TeV.

A particular spots of CMS program at 13 TeV would be a detailed study of heavy flavour production that was statistically limited till now. While Z+b is known to be a channel more sensitive to the flavour scheme used in PDF evolution than the PDF content itself, W+c was demostrated to provide an impact on strageness content of the proton. Finally the Z or γ+c and W+b channels are expected to provide for the first time constraints for the intrinsic charm content of the proton [150]. Finally while the potential of $t\bar{t}$ differential production to constraint the gluon PDF was demostrated at 8 TeV a statistically larger sample is required to make a sizeable impact on PDFs.

The collaboration plan to maintain the effort and expertise to extend the tests of α_s running in the multi-TeV range. In particular the dijet production is expected to be measured triple-differentially in m_{jj}, y_{j1} and y_{j2}. This setup was proposed by the authors of Ref. [70] to take the best advantage of the NNLO calculations once they would be public for the α_s and PDF extraction.

5.3 Prospects from LHCb

LHCb will continue to make a number of measurements relevant for constraining PDFs in Run-II. The increased centre-of-mass energy extends the kinematic range of the experiment to lower x values for W, Z and low-mass Drell-Yan production. Larger cross-sections are also expected in Run-II for the production of W and Z bosons in association with heavy quarks. As the precision of current Run-1 measurements is limited by the available statistics [146, 147], more precise measurements can be expected in Run-II. In particular measurements of W production in association with charm jets or D mesons will provide information on the strange content of the proton complementary to that from ATLAS and CMS.

The greater centre-of-mass energy in Run-II will also result in a dramatic increase in the $t\bar{t}$ production cross-section in the LHCb fiducial region. Consequently measurements of $t\bar{t}$ production can be made with a much improved statistical precision in Run-II at LHCb. Such a measurement, originally proposed in the context of the forward-backward asymmetry [151], will provide important information on the large-x gluon PDF [152].

In addition to extending coverage to an even lower x-region, measurements of $b\bar{b}$ and $c\bar{c}$ production in Run-II will allow a determination of the production ratio of heavy quarks at different centre of mass energies. The relatively large theoretical uncertainties present in the predictions for these processes make the ratios particularly attractive as a partial cancellation is expected. As such, the ratios may provide more stringent constraints on the PDFs than the individual measurements.

The installation of a dedicated forward shower counter system (HERSCHEL) either side of the LHCb detector ahead of Run-II has the potential to improve the precision of measurements of central exclusive production by extending the LHCb coverage into the

very forward region. Current LHCb measurements of exclusive J/ψ and $\psi(2S)$ production [149] contain large backgrounds arising from inelastic production where the disociation of one or both protons is not detected. HERSCHEL allows such events to be rejected by identifying forward showers through the interaction of high rapidity particles with the beam pipe. Consequently, a higher purity and precision can be expected for Run-II measurements.

6 Summary and outlook

In this document we have summarized the constraints on PDFs that have been obtained from Run I LHC measurements, and reviewed the prospects to the upcoming 13 TeV Run II data-taking. We hope that this note can be useful both for the LHC collaborations, in order to identify their priorities for PDF-sensitive measurements at Run II, as well as to the PDF collaborations, to have a clear perspective of which measurements are available and which ones will also become available in the near future.

In this paper we have concentrated only on the experimental constraints provided by the LHC data. Equally important for PDF determinations is to use state-of-the-art theoretical calculations, and their benchmarking between PDF fitting groups. At the level of structure functions, this benchmarking has been performed in a number of studies [153, 154], and would be desirable to continue these systematic comparisons also for hadronic observables. This is specially important now that the requirements of LHC data make higher order QCD and electroweak calculations essential for PDF analysis.

Also, in this report we have not examined differences and similarities between recent PDF fits, nor explored which ones should be preferably used in the LHC data analysis. This will be the subject of a companion PDF4LHC report.

Acknowledgments

We are specially grateful to Jose Ignacio Latorre and all the Pedro Pascual Benasque Center for Science team for their invaluable support during the workshop *Parton Distributions for the LHC* in February 2015, where many of the authors of this paper were present.

References

[1] S. Forte, *Parton distributions at the dawn of the LHC*, *Acta Phys.Polon.* **B41** (2010) 2859–2920, [arXiv:1011.5247].

[2] S. Forte and G. Watt, *Progress in the Determination of the Partonic Structure of the Proton*, *Ann.Rev.Nucl.Part.Sci.* **63** (2013) 291–328, [arXiv:1301.6754].

[3] E. Perez and E. Rizvi, *The Quark and Gluon Structure of the Proton*, *Rep.Prog.Phys.* **76** (2013) 046201, [arXiv:1208.1178].

[4] R. D. Ball, S. Carrazza, L. Del Debbio, S. Forte, J. Gao, et al., *Parton Distribution Benchmarking with LHC Data*, *JHEP* **1304** (2013) 125, [arXiv:1211.5142].

[5] G. Watt, *Parton distribution function dependence of benchmark Standard Model total cross sections at the 7 TeV LHC*, *JHEP* **1109** (2011) 069, [arXiv:1106.5788].

[6] A. De Roeck and R. Thorne, *Structure Functions*, *Prog.Part.Nucl.Phys.* **66** (2011) 727–781, [arXiv:1103.0555].

[7] **LHC Higgs Cross Section Working Group** Collaboration, S. Dittmaier et al., *Handbook of LHC Higgs Cross Sections: 1. Inclusive Observables*, arXiv:1101.0593.

[8] **LHeC Study Group** Collaboration, J. Abelleira Fernandez et al., *A Large Hadron Electron Collider at CERN: Report on the Physics and Design Concepts for Machine and Detector*, *J.Phys.* **G39** (2012) 075001, [arXiv:1206.2913].

[9] C. Borschensky, M. Krmer, A. Kulesza, M. Mangano, S. Padhi, et al., *Squark and gluino production cross sections in pp collisions at $\sqrt{s}$ = 13, 14, 33 and 100 TeV*, arXiv:1407.5066.

[10] G. Bozzi, J. Rojo, and A. Vicini, *The Impact of PDF uncertainties on the measurement of the W boson mass at the Tevatron and the LHC*, *Phys.Rev.* **D83** (2011) 113008, [arXiv:1104.2056].

[11] **ATLAS** Collaboration, G. Aad et al., *Studies of theoretical uncertainties on the measurement of the mass of the W boson at the LHC*, ATL-PHYS-PUB-2014-015.

[12] G. Bozzi, L. Citelli, and A. Vicini, *PDF uncertainties on the W boson mass measurement from the lepton transverse momentum distribution*, arXiv:1501.0558.

[13] S. Alekhin, J. Bluemlein, and S. Moch, *The ABM parton distributions tuned to LHC data*, *Phys.Rev.* **D89** (2014) 054028, [arXiv:1310.3059].

[14] J. Gao, M. Guzzi, J. Huston, H.-L. Lai, Z. Li, et al., *The CT10 NNLO Global Analysis of QCD*, arXiv:1302.6246.

[15] **ZEUS , H1** Collaboration, A. Cooper-Sarkar, *PDF Fits at HERA*, *PoS* **EPS-HEP2011** (2011) 320, [arXiv:1112.2107].

[16] L. Harland-Lang, A. Martin, P. Motylinski, and R. Thorne, *Parton distributions in the LHC era: MMHT 2014 PDFs*, arXiv:1412.3989.

[17] **The NNPDF Collaboration** Collaboration, R. D. Ball et al., *Parton distributions for the LHC Run II*, arXiv:1410.8849.

[18] B. Watt, P. Motylinski, and R. Thorne, *The Effect of LHC Jet Data on MSTW PDFs*, *Eur.Phys.J.* **C74** (2014) 2934, [arXiv:1311.5703].

[19] **ATLAS** Collaboration, G. Aad et al., *Measurement of the inclusive jet cross section in pp collisions at sqrt(s)=2.76 TeV and comparison to the inclusive jet cross section at sqrt(s)=7 TeV using the ATLAS detector*, *Eur.Phys.J.* **C73** (2013) 2509, [arXiv:1304.4739].

[20] **CMS** Collaboration, S. Chatrchyan et al., *Measurements of differential jet cross sections in proton-proton collisions at $\sqrt{s} = 7$ TeV with the CMS detector*, *Phys.Rev.* **D87** (2013) 112002, [arXiv:1212.6660].

[21] **CMS** Collaboration, S. Chatrchyan et al., *Measurement of the muon charge asymmetry in inclusive pp to WX production at sqrt(s) = 7 TeV and an improved determination of light parton distribution functions*, *Phys.Rev.* **D90** (2014) 032004, [arXiv:1312.6283].

[22] **ATLAS** Collaboration, G. Aad et al., *Determination of the strange quark density of the proton from ATLAS measurements of the W, Z cross sections*, *Phys.Rev.Lett.* (2012) [arXiv:1203.4051].

[23] D. d'Enterria and J. Rojo, *Quantitative constraints on the gluon distribution function in the proton from collider isolated-photon data*, *Nucl.Phys.* **B860** (2012) 311–338, [arXiv:1202.1762].

[24] **CMS Collaboration** Collaboration, S. Chatrchyan et al., *Measurement of associated W + charm production in pp collisions at $\sqrt{s} = 7$ TeV*, *JHEP* **1402** (2014) 013, [arXiv:1310.1138].

[25] **ATLAS** Collaboration, G. Aad et al., *Measurement of the production of a W boson in association with a charm quark in pp collisions at $\sqrt{s} = 7$ TeV with the ATLAS detector*, *JHEP* **1405** (2014) 068, [arXiv:1402.6263].

[26] S. Alekhin, J. Bluemlein, L. Caminadac, K. Lipka, K. Lohwasser, et al., *Determination of Strange Sea Quark Distributions from Fixed-target and Collider Data*, arXiv:1404.6469.

[27] M. Czakon, M. L. Mangano, A. Mitov, and J. Rojo, *Constraints on the gluon PDF from top quark pair production at hadron colliders*, *JHEP* **1307** (2013) 167, [arXiv:1303.7215].

[28] M. Guzzi, K. Lipka, and S.-O. Moch, *Top-quark pair production at hadron colliders: differential cross section and phenomenological applications with DiffTop*, *JHEP* **1501** (2015) 082, [arXiv:1406.0386].

[29] O. Zenaiev, A. Geiser, K. Lipka, J. Blmlein, A. Cooper-Sarkar, et al., *Impact of heavy-flavour production cross sections measured by the LHCb experiment on parton distribution functions at low x*, arXiv:1503.0458.

[30] **LHCb** Collaboration, R. Aaij et al., *Prompt charm production in pp collisions at sqrt(s)=7 TeV*, *Nucl.Phys.* **B871** (2013) 1–20, [arXiv:1302.2864].

[31] **CMS Collaboration** Collaboration, S. Chatrchyan et al., *Measurement of the differential and double-differential Drell-Yan cross sections in proton-proton collisions at $\sqrt{s}$ = 7 TeV*, *JHEP* **1312** (2013) 030, [arXiv:1310.7291].

[32] **ATLAS** Collaboration, G. Aad et al., *Measurement of the high-mass Drell–Yan differential cross-section in pp collisions at $\sqrt{s}$=7 TeV with the ATLAS detector*, *Phys.Lett.* **B725** (2013) 223–242, [arXiv:1305.4192].

[33] S. A. Malik and G. Watt, *Ratios of W and Z cross sections at large boson p_T as a constraint on PDFs and background to new physics*, *JHEP* **1402** (2014) 025, [arXiv:1304.2424].

[34] W. Stirling and E. Vryonidou, *Charm production in association with an electroweak gauge boson at the LHC*, *Phys.Rev.Lett.* **109** (2012) 082002, [arXiv:1203.6781].

[35] D. Mason et al., *Measurement of the Nucleon Strange-Antistrange Asymmetry at Next-to-Leading Order in QCD from NuTeV Dimuon Data*, *Phys. Rev. Lett.* **99** (2007) 192001.

[36] M. Beneke, P. Falgari, S. Klein, J. Piclum, C. Schwinn, et al., *Inclusive Top-Pair Production Phenomenology with TOPIXS*, *JHEP* **1207** (2012) 194, [arXiv:1206.2454].

[37] M. L. Mangano and J. Rojo, *Cross Section Ratios between different CM energies at the LHC: opportunities for precision measurements and BSM sensitivity*, *JHEP* **1208** (2012) 010, [arXiv:1206.3557].

[38] **CMS Collaboration** Collaboration, V. Khachatryan et al., *Measurements of differential and double-differential Drell-Yan cross sections in proton-proton collisions at $\sqrt{s}$ = 8 TeV*, arXiv:1412.1115.

[39] P. Skands, S. Carrazza, and J. Rojo, *Tuning PYTHIA 8.1: the Monash 2013 Tune*, *European Physical Journal* **74** (2014) 3024, [arXiv:1404.5630].

[40] **ATLAS** Collaboration, G. Aad et al., *ATLAS Run 1 Pythia8 tunes*, ATL-PHYS-PUB-2014-021.

[41] **CMS Collaboration** Collaboration, V. Khachatryan et al., *Constraints on parton distribution functions and extraction of the strong coupling constant from the inclusive jet cross section in pp collisions at $\sqrt{s}$ = 7 TeV*, arXiv:1410.6765.

[42] **CMS** Collaboration, S. Chatrchyan et al., *Measurement of the ratio of the inclusive 3-jet cross section to the inclusive 2-jet cross section in pp collisions at $\sqrt{s}$ = 7 TeV and first determination of the strong coupling constant in the TeV range*, *Eur.Phys.J.* **C73** (2013), no. 10 2604, [arXiv:1304.7498].

[43] S. Alekhin, O. Behnke, P. Belov, S. Borroni, M. Botje, et al., *HERAFitter, Open Source QCD Fit Project*, arXiv:1410.4412.

[44] **HERAFitter developers' Team** Collaboration, S. Camarda et al., *QCD analysis of W- and Z-boson production at Tevatron*, arXiv:1503.0522.

[45] **HERAFitter developers' Team** Collaboration, P. Belov et al., *Parton distribution functions at LO, NLO and NNLO with correlated uncertainties between orders*, *Eur.Phys.J.* **C74** (2014), no. 10 3039, [arXiv:1404.4234].

[46] J. Gao and P. Nadolsky, *A meta-analysis of parton distribution functions*, *JHEP* **1407** (2014) 035, [arXiv:1401.0013].

[47] S. Alekhin, S. Alioli, R. D. Ball, V. Bertone, J. Blumlein, et al., *The PDF4LHC Working Group Interim Report*, arXiv:1101.0536.

[48] M. Botje et al., *The PDF4LHC Working Group Interim Recommendations*, arXiv:1101.0538.

[49] V. Bertone, S. Carrazza, and J. Rojo, *APFEL: A PDF Evolution Library with QED corrections*, *Comput.Phys.Commun.* **185** (2014) 1647–1668, [arXiv:1310.1394].

[50] S. Carrazza, A. Ferrara, D. Palazzo, and J. Rojo, *APFEL Web: a web-based application for the graphical visualization of parton distribution functions*, arXiv:1410.5456.

[51] A. D. Martin, W. J. Stirling, R. S. Thorne, and G. Watt, *Parton distributions for the LHC*, *Eur. Phys. J.* **C63** (2009) 189–285, [arXiv:0901.0002].

[52] A. Martin, A. T. Mathijssen, W. Stirling, R. Thorne, B. Watt, et al., *Extended Parameterisations for MSTW PDFs and their effect on Lepton Charge Asymmetry from W Decays*, *Eur.Phys.J.* **C73** (2013), no. 2 2318, [arXiv:1211.1215].

[53] J. Owens, A. Accardi, and W. Melnitchouk, *Global parton distributions with nuclear and finite-Q^2 corrections*, arXiv:1212.1702.

[54] R. Thorne, *The Effect of Changes of Variable Flavour Number Scheme on PDFs and Predicted Cross Sections*, *Phys. Rev.* **D86** (2012) 074017, [arXiv:1201.6180].

[55] D. de Florian, R. Sassot, P. Zurita, and M. Stratmann, *Global Analysis of Nuclear Parton Distributions*, *Phys.Rev.* **D85** (2012) 074028, [arXiv:1112.6324].

[56] **The NNPDF** Collaboration, R. D. Ball et al., *Fitting Parton Distribution Data with Multiplicative Normalization Uncertainties*, *JHEP* **05** (2010) 075, [arXiv:0912.2276].

[57] **H1 and ZEUS** Collaboration, F. Aaron et al., *Combined Measurement and QCD Analysis of the Inclusive e+- p Scattering Cross Sections at HERA*, *JHEP* **1001** (2010) 109, [arXiv:0911.0884].

[58] **H1 , ZEUS** Collaboration, H. Abramowicz et al., *Combination and QCD Analysis of Charm Production Cross Section Measurements in Deep-Inelastic ep Scattering at HERA*, *Eur.Phys.J.* **C73** (2013) 2311, [arXiv:1211.1182].

[59] **CDF , D0** Collaboration, T. A. Aaltonen et al., *Combination of measurements of the top-quark pair production cross section from the Tevatron Collider*, *Phys.Rev.* **D89** (2014) 072001, [arXiv:1309.7570].

[60] **NNPDF** Collaboration, R. D. Ball, V. Bertone, S. Carrazza, C. S. Deans, L. Del Debbio, et al., *Parton distributions with LHC data*, *Nucl.Phys.* **B867** (2013) 244–289, [arXiv:1207.1303].

[61] V. Bertone, R. Frederix, S. Frixione, J. Rojo, and M. Sutton, *aMCfast: automation of fast NLO computations for PDF fits*, *JHEP* **1408** (2014) 166, [arXiv:1406.7693].

[62] **fastNLO** Collaboration, M. Wobisch, D. Britzger, T. Kluge, K. Rabbertz, and F. Stober, *Theory-Data Comparisons for Jet Measurements in Hadron-Induced Processes*, arXiv:1109.1310.

[63] T. Carli, D. Clements, A. Cooper-Sarkar, C. Gwenlan, G. P. Salam, et al., *A posteriori inclusion of parton density functions in NLO QCD final-state calculations at hadron colliders: The APPLGRID Project*, *Eur.Phys.J.* **C66** (2010) 503–524, [arXiv:0911.2985].

[64] D. de Florian, P. Hinderer, A. Mukherjee, F. Ringer, and W. Vogelsang, *Approximate next-to-next-to-leading order corrections to hadronic jet production*, *Phys.Rev.Lett.* **112** (2014) 082001, [arXiv:1310.7192].

[65] S. Carrazza and J. Pires, *Perturbative QCD description of jet data from LHC Run-I and Tevatron Run-II*, arXiv:1407.7031.

[66] A. Gehrmann-De Ridder, T. Gehrmann, E. Glover, and J. Pires, *Second order QCD corrections to jet production at hadron colliders: the all-gluon contribution*, *Phys.Rev.Lett.* **110** (2013) 162003, [arXiv:1301.7310].

[67] S. Forte, E. Laenen, P. Nason, and J. Rojo, *Heavy quarks in deep-inelastic scattering*, *Nucl. Phys.* **B834** (2010) 116–162, [arXiv:1001.2312].

[68] **H1 and ZEUS** Collaboration.

[69] J. Rojo, *Constraints on parton distributions and the strong coupling from LHC jet data*, arXiv:1410.7728.

[70] J. Currie, A. Gehrmann-De Ridder, E. Glover, and J. Pires, *NNLO QCD corrections to jet production at hadron colliders from gluon scattering*, *JHEP* **1401** (2014) 110, [arXiv:1310.3993].

[71] **The NNPDF** Collaboration, R. D. Ball et al., *A first unbiased global NLO determination of parton distributions and their uncertainties*, *Nucl. Phys.* **B838** (2010) 136–206, [arXiv:1002.4407].

[72] L. Carminati, G. Costa, D. D'Enterria, I. Koletsou, G. Marchiori, et al., *Sensitivity of the LHC isolated-gamma+jet data to the parton distribution functions of the proton*, *Europhys.Lett.* **101** (2013) 61002, [arXiv:1212.5511].

[73] **ATLAS** Collaboration, G. Aad et al., *A study of the sensitivity to the proton parton distributions of the inclusive photon production cross section in pp collisions at 7 TeV measured by the ATLAS experiment at the LHC*, .

[74] **ATLAS** Collaboration, G. Aad et al., *Measurement of the inclusive W+- and Z/gamma cross sections in the electron and muon decay channels in pp collisions at sqrt(s) = 7 TeV with the ATLAS detector*, *Phys.Rev.* **D85** (2012) 072004, [arXiv:1109.5141].

[75] S. Marzani and R. D. Ball, *High Energy Resummation of Drell-Yan Processes*, *Nucl.Phys.* **B814** (2009) 246–264, [arXiv:0812.3602].

[76] R. Gavin, Y. Li, F. Petriello, and S. Quackenbush, *W Physics at the LHC with FEWZ 2.1*, *Comput.Phys.Commun.* **184** (2013) 208–214, [arXiv:1201.5896].

[77] R. Boughezal, Y. Li, and F. Petriello, *Disentangling radiative corrections using high-mass Drell-Yan at the LHC*, *Phys.Rev.* **D89** (2014) 034030, [arXiv:1312.3972].

[78] **NNPDF** Collaboration, R. D. Ball et al., *Parton distributions with QED corrections*, *Nucl.Phys.* **B877** (2013) 290–320, [arXiv:1308.0598].

[79] A. D. Martin, R. G. Roberts, W. J. Stirling, and R. S. Thorne, *Parton distributions incorporating QED contributions*, *Eur. Phys. J.* **C39** (2005) 155–161, [hep-ph/0411040].

[80] **ATLAS** Collaboration, G. Aad et al., *Measurement of the Z/γ^* boson transverse momentum distribution in pp collisions at $\sqrt{s}$ = 7 TeV with the ATLAS detector*, *JHEP* **1409** (2014) 145, [arXiv:1406.3660].

[81] U. Baur, F. Halzen, S. Keller, M. L. Mangano, and K. Riesselmann, *The Charm content of W + 1 jet events as a probe of the strange quark distribution function*, *Phys.Lett.* **B318** (1993) 544–548, [hep-ph/9308370].

[82] M. Czakon, P. Fiedler, and A. Mitov, *The total top quark pair production cross-section at hadron colliders through $O(\alpha_S^4)$*, *Phys.Rev.Lett.* **110** (2013) 252004, [arXiv:1303.6254].

[83] M. Czakon, P. Fiedler, and A. Mitov, *Resolving the Tevatron top quark forward-backward asymmetry puzzle*, arXiv:1411.3007.

[84] **CMS** Collaboration, S. Chatrchyan et al., *Determination of the top-quark pole mass and strong coupling constant from the t t-bar production cross section in pp collisions at $\sqrt{s}$ = 7 TeV*, *Phys.Lett.* **B728** (2014) 496–517, [arXiv:1307.1907].

[85] S. Jones, A. Martin, M. Ryskin, and T. Teubner, *Probes of the small x gluon via exclusive J/ψ and Υ production at HERA and the LHC*, *JHEP* **1311** (2013) 085, [arXiv:1307.7099].

[86] S. Jones, A. Martin, M. Ryskin, and T. Teubner, *Predictions of exclusive (2S) production at the LHC*, *J.Phys.* **G41** (2014) 055009, [arXiv:1312.6795].

[87] **ATLAS Collaboration** Collaboration, G. Aad et al., *Measurement of the low-mass Drell-Yan differential cross section at $\sqrt{s} = 7$ TeV using the ATLAS detector*, *JHEP* **1406** (2014) 112, [arXiv:1404.1212].

[88] **ATLAS** Collaboration, G. Aad et al., *Measurement of the forward-backward asymmetry of electron and muon pair-production in pp collisions at $\sqrt{s} = 7$ TeV with the ATLAS detector*, arXiv:1503.0370.

[89] **ATLAS** Collaboration, G. Aad et al., *Measurement of the cross section for the production of a W boson in association with b^- jets in pp collisions at $\sqrt{s} = 7$ TeV with the ATLAS detector*, *Phys.Lett.* **B707** (2012) 418–437, [arXiv:1109.1470].

[90] **ATLAS** Collaboration, G. Aad et al., *Measurement of the cross-section for W boson production in association with b-jets in pp collisions at $\sqrt{s} = 7$ TeV with the ATLAS detector*, *JHEP* **1306** (2013) 084, [arXiv:1302.2929].

[91] **ATLAS** Collaboration, G. Aad et al., *Measurement of the cross-section for b^- jets produced in association with a Z boson at $\sqrt{s} = 7$ TeV with the ATLAS detector*, *Phys.Lett.* **B706** (2012) 295–313, [arXiv:1109.1403].

[92] **ATLAS** Collaboration, G. Aad et al., *Measurement of differential production cross-sections for a Z boson in association with b-jets in 7 TeV proton-proton collisions with the ATLAS detector*, *JHEP* **1410** (2014) 141, [arXiv:1407.3643].

[93] **ATLAS** Collaboration, G. Aad et al., *Measurement of the transverse momentum distribution of Z/gamma* bosons in proton-proton collisions at $\sqrt{s} = 7$ TeV with the ATLAS detector*, *Phys.Lett.* **B705** (2011) 415–434, [arXiv:1107.2381].

[94] **ATLAS** Collaboration, G. Aad et al., *Measurement of the Transverse Momentum Distribution of W Bosons in pp Collisions at $\sqrt{s} = 7$ TeV with the ATLAS Detector*, *Phys.Rev.* **D85** (2012) 012005, [arXiv:1108.6308].

[95] **ATLAS** Collaboration, G. Aad et al., *Measurement of the production cross section for Z/gamma* in association with jets in pp collisions at $\sqrt{s} = 7$ TeV with the ATLAS detector*, *Phys.Rev.* **D85** (2012) 032009, [arXiv:1111.2690].

[96] **ATLAS** Collaboration, G. Aad et al., *Measurement of the production cross section of jets in association with a Z boson in pp collisions at $\sqrt{s} = 7$ TeV with the ATLAS detector*, *JHEP* **1307** (2013) 032, [arXiv:1304.7098].

[97] **ATLAS** Collaboration, G. Aad et al., *Study of jets produced in association with a W boson in pp collisions at $\sqrt{s} = 7$ TeV with the ATLAS detector*, *Phys.Rev.* **D85** (2012) 092002, [arXiv:1201.1276].

[98] **ATLAS** Collaboration, G. Aad et al., *Measurements of the W production cross sections in association with jets with the ATLAS detector*, *Eur.Phys.J.* **C75** (2015), no. 2 82, [arXiv:1409.8639].

[99] **ATLAS** Collaboration, G. Aad et al., *A measurement of the ratio of the production cross sections for W and Z bosons in association with jets with the ATLAS detector*, *Eur.Phys.J.* **C74** (2014), no. 12 3168, [arXiv:1408.6510].

[100] **ATLAS** Collaboration, G. Aad et al., *Measurement of inclusive jet and dijet production in pp collisions at sqrt(s) = 7 TeV using the ATLAS detector*, *Phys. Rev.* **D86** (2012) 014022, [arXiv:1112.6297].

[101] **ATLAS Collaboration** Collaboration, G. Aad et al., *Measurement of the inclusive jet cross-section in proton-proton collisions at $\sqrt{s} = 7$ TeV using 4.5 fb^{-1} of data with the ATLAS detector*, arXiv:1410.8857.

[102] **ATLAS Collaboration** Collaboration, G. Aad et al., *Measurement of dijet cross sections in pp collisions at 7 TeV centre-of-mass energy using the ATLAS detector*, *JHEP* **1405** (2014) 059, [arXiv:1312.3524].

[103] **ATLAS Collaboration** Collaboration, G. Aad et al., *Measurement of three-jet production cross-sections in pp collisions at 7 TeV centre-of-mass energy using the ATLAS detector*, arXiv:1411.1855.

[104] **ATLAS** Collaboration, G. Aad et al., *Measurement of the inclusive isolated prompt photon cross-section in pp collisions at $\sqrt{s} = 7$ TeV using 35 pb-1 of ATLAS data*, *Phys.Lett.* **B706** (2011) 150–167, [arXiv:1108.0253].

[105] **ATLAS** Collaboration, G. Aad et al., *Measurement of the inclusive isolated prompt photons cross section in pp collisions at $\sqrt{s} = 7$TeV with the ATLAS detector using 4.6fb^1*, *Phys.Rev.* **D89** (2014), no. 5 052004, [arXiv:1311.1440].

[106] **ATLAS** Collaboration, G. Aad et al., *Measurement of the production cross section of an isolated photon associated with jets in proton-proton collisions at $\sqrt{s} = 7$ TeV with the ATLAS detector*, *Phys.Rev.* **D85** (2012) 092014, [arXiv:1203.3161].

[107] **ATLAS** Collaboration, G. Aad et al., *Measurement of the top quark-pair production cross section with ATLAS in pp collisions at $\sqrt{s} = 7$ TeV*, *Eur.Phys.J.* **C71** (2011) 1577, [arXiv:1012.1792].

[108] **ATLAS** Collaboration, G. Aad et al., *Measurement of the top quark pair production cross section in pp collisions at $\sqrt{s} = 7$ TeV in dilepton final states with ATLAS*, *Phys.Lett.* **B707** (2012) 459–477, [arXiv:1108.3699].

[109] **ATLAS** Collaboration, G. Aad et al., *Measurement of the top quark pair production cross-section with ATLAS in the single lepton channel*, *Phys.Lett.* **B711** (2012) 244–263, [arXiv:1201.1889].

[110] **ATLAS** Collaboration, G. Aad et al., *Measurement of the cross section for top-quark pair production in pp collisions at $\sqrt{s} = 7$ TeV with the ATLAS detector*

using final states with two high-pt leptons, *JHEP* **1205** (2012) 059, [arXiv:1202.4892].

[111] **ATLAS** Collaboration, G. Aad et al., *Measurement of the top quark pair cross section with ATLAS in pp collisions at sqrt(s) = 7 TeV using final states with an electron or a muon and a hadronically decaying τ lepton*, *Phys.Lett.* **B717** (2012) 89–108, [arXiv:1205.2067].

[112] **ATLAS** Collaboration, G. Aad et al., *Measurement of the ttbar production cross section in the tau+jets channel using the ATLAS detector*, *Eur.Phys.J.* **C73** (2013), no. 3 2328, [arXiv:1211.7205].

[113] **ATLAS** Collaboration, G. Aad et al., *Measurement of the $t\bar{t}$ production cross-section using $e\mu$ events with b -tagged jets in pp collisions at $\sqrt{s} = 7$ and 8 TeV with the ATLAS detector*, *Eur.Phys.J.* **C74** (2014), no. 10 3109, [arXiv:1406.5375].

[114] **ATLAS** Collaboration, G. Aad et al., *Measurements of top quark pair relative differential cross-sections with ATLAS in pp collisions at $\sqrt{s} = 7$ TeV*, *Eur.Phys.J.* **C73** (2013), no. 1 2261, [arXiv:1207.5644].

[115] **ATLAS** Collaboration, G. Aad et al., *Measurements of normalized differential cross sections for $t\bar{t}$ production in pp collisions at $\sqrt{s} = 7$TeV using the ATLAS detector*, *Phys.Rev.* **D90** (2014), no. 7 072004, [arXiv:1407.0371].

[116] **ATLAS** Collaboration, G. Aad et al., *Simultaneous measurements of the $t\bar{t}$, W^+W^-, and $Z/\gamma^* \to \tau\tau$ production cross-sections in pp collisions at $\sqrt{s} = 7$ TeV with the ATLAS detector*, *Phys.Rev.* **D91** (2015), no. 5 052005, [arXiv:1407.0573].

[117] M. Cacciari, G. P. Salam, and G. Soyez, *The Anti-k(t) jet clustering algorithm*, *JHEP* **0804** (2008) 063, [arXiv:0802.1189].

[118] F. Maltoni, G. Ridolfi, and M. Ubiali, *b-initiated processes at the LHC: a reappraisal*, *JHEP* **1207** (2012) 022, [arXiv:1203.6393].

[119] **CMS** Collaboration, S. Chatrchyan et al., *Forward-backward asymmetry of Drell-Yan lepton pairs in pp collisions at $\sqrt{s} = 7$ TeV*, *Phys.Lett.* **B718** (2013) 752–772, [arXiv:1207.3973].

[120] **CMS** Collaboration, S. Chatrchyan et al., *Measurement of the lepton charge asymmetry in inclusive W production in pp collisions at $\sqrt{s} = 7$ TeV*, *JHEP* **1104** (2011) 050, [arXiv:1103.3470].

[121] **CMS** Collaboration, S. Chatrchyan et al., *Measurement of the electron charge asymmetry in inclusive W production in pp collisions at sqrt(s) = 7 TeV*, *Phys.Rev.Lett.* **109** (2012) 111806, [arXiv:1206.2598].

[122] **CMS** Collaboration, V. Khachatryan et al., *Measurements of Inclusive W and Z Cross Sections in pp Collisions at $\sqrt{s} = 7$ TeV*, *JHEP* **1101** (2011) 080, [arXiv:1012.2466].

[123] **CMS** Collaboration, S. Chatrchyan et al., *Measurement of the Inclusive W and Z Production Cross Sections in pp Collisions at $\sqrt{s} = 7$ TeV*, *JHEP* **1110** (2011) 132, [arXiv:1107.4789].

[124] **CMS** Collaboration, S. Chatrchyan et al., *Measurement of inclusive W and Z boson production cross sections in pp collisions at $\sqrt{s} = 8$ TeV*, *Phys.Rev.Lett.* **112** (2014) 191802, [arXiv:1402.0923].

[125] **CMS** Collaboration, S. Chatrchyan et al., *Measurement of the Rapidity and Transverse Momentum Distributions of Z Bosons in pp Collisions at $\sqrt{s} = 7$ TeV*, *Phys.Rev.* **D85** (2012) 032002, [arXiv:1110.4973].

[126] **CMS** Collaboration, S. Chatrchyan et al., *Measurement of the ratio of inclusive jet cross sections using the anti-k_T algorithm with radius parameters R=0.5 and 0.7 in pp collisions at $\sqrt{s} = 7$TeV*, *Phys.Rev.* **D90** (2014), no. 7 072006, [arXiv:1406.0324].

[127] **CMS Collaboration** Collaboration, V. Khachatryan et al., *Measurement of the inclusive 3-jet production differential cross section in proton-proton collisions at 7 TeV and determination of the strong coupling constant in the TeV range*, arXiv:1412.1633.

[128] **CMS** Collaboration, S. Chatrchyan et al., *Measurement of the production cross sections for a Z boson and one or more b jets in pp collisions at sqrt(s) = 7 TeV*, *JHEP* **1406** (2014) 120, [arXiv:1402.1521].

[129] **CMS** Collaboration, S. Chatrchyan et al., *Measurement of the Differential Cross Section for Isolated Prompt Photon Production in pp Collisions at 7 TeV*, *Phys.Rev.* **D84** (2011) 052011, [arXiv:1108.2044].

[130] **CMS** Collaboration, S. Chatrchyan et al., *Measurement of the triple-differential cross section for photon+jets production in proton-proton collisions at $\sqrt{s}$=7 TeV*, *JHEP* **1406** (2014) 009, [arXiv:1311.6141].

[131] **CMS** Collaboration, S. Chatrchyan et al., *Measurement of the $t\bar{t}$ production cross section in the dilepton channel in pp collisions at $\sqrt{s} = 7$ TeV*, *JHEP* **1211** (2012) 067, [arXiv:1208.2671].

[132] **CMS** Collaboration, S. Chatrchyan et al., *Measurement of differential top-quark pair production cross sections in pp colisions at $\sqrt{s} = 7$ TeV*, *Eur.Phys.J.* **C73** (2013) 2339, [arXiv:1211.2220].

[133] **CMS** Collaboration, C. Collaboration, *Top pair cross section in dileptons, CMS-PAS-TOP-11-005*, .

[134] **CMS** Collaboration, CMS, *Top pair cross section in e/mu+jets at 8 TeV*, .

[135] **CMS** Collaboration, CMS, *Top pair cross section in dileptons*, .

[136] A. D. Martin, R. G. Roberts, W. J. Stirling, and R. S. Thorne, *Uncertainties of predictions from parton distributions. I: Experimental errors. ((T))*, *Eur. Phys. J.* **C28** (2003) 455–473, [hep-ph/0211080].

[137] D. Becciolini, M. Gillioz, M. Nardecchia, F. Sannino, and M. Spannowsky, *Constraining new colored matter from the ratio of 3 to 2 jets cross sections at the LHC*, *Phys.Rev.* **D91** (2015), no. 1 015010, [arXiv:1403.7411].

[138] **CMS** Collaboration, S. Chatrchyan et al., *Measurement of the weak mixing angle with the Drell-Yan process in proton-proton collisions at the LHC*, *Phys.Rev.* **D84** (2011) 112002, [arXiv:1110.2682].

[139] R. Thorne, A. Martin, W. Stirling, and G. Watt, *Parton Distributions and QCD at LHCb*, arXiv:0808.1847.

[140] **LHCb Collaboration** Collaboration, R. Aaij et al., *Inclusive W and Z production in the forward region at $\sqrt{s} = 7$ TeV*, *JHEP* **1206** (2012) 058, [arXiv:1204.1620].

[141] **LHCb collaboration** Collaboration, R. Aaij et al., *Measurement of the cross-section for $Z \to e^+e^-$ production in pp collisions at $\sqrt{s} = 7$ TeV*, *JHEP* **1302** (2013) 106, [arXiv:1212.4620].

[142] **LHCb** Collaboration, R. Aaij et al., *Measurement of the forward W boson cross-section in pp collisions at $\sqrt{s} = 7$ TeV*, *JHEP* **1412** (2014) 079, [arXiv:1408.4354].

[143] **LHCb** Collaboration, R. Aaij et al., *Precision luminosity measurements at LHCb*, *JINST* **9** (2014), no. 12 P12005, [arXiv:1410.0149].

[144] **LHCb** Collaboration, R. Aaij et al., *Measurement of forward $\mathrm{Z} \to \mathrm{e}^+\mathrm{e}^-$ production at $\sqrt{s} = 8$ TeV*, arXiv:1503.0096.

[145] **LHCb** Collaboration, "Inclusive low mass Drell-Yan production in the forward region at $\sqrt{s} = 7$ TeV." Linked to LHCb-ANA-2012-029, Mar, 2012.

[146] **LHCb** Collaboration, R. Aaij et al., *Measurement of the Z+b-jet cross-section in pp collisions at $\sqrt{s} = 7$ TeV in the forward region*, *JHEP* **1501** (2015) 064, [arXiv:1411.1264].

[147] **LHCb** Collaboration, R. Aaij et al., *Observation of associated production of a Z boson with a D meson in the forward region*, *JHEP* **1404** (2014) 091, [arXiv:1401.3245].

[148] **LHCb** Collaboration, R. Aaij et al., *Measurement of B meson production cross-sections in proton-proton collisions at $\sqrt{s} = 7$ TeV*, *JHEP* **1308** (2013) 117, [arXiv:1306.3663].

[149] **LHCb collaboration** Collaboration, R. Aaij et al., *Updated measurements of exclusive J/ and (2S) production cross-sections in pp collisions at $\sqrt{s} = 7$ TeV*, *J.Phys.* **G41** (2014) 055002, [arXiv:1401.3288].

[150] V. Bednyakov, M. Demichev, G. Lykasov, T. Stavreva, and M. Stockton, *Searching for intrinsic charm in the proton at the LHC*, *EPJ Web Conf.* **60** (2013) 20047, [arXiv:1305.3548].

[151] A. L. Kagan, J. F. Kamenik, G. Perez, and S. Stone, *Top LHCb Physics*, *Phys.Rev.Lett.* **107** (2011) 082003, [arXiv:1103.3747].

[152] R. Gauld, *Feasibility of top quark measurements at LHCb and constraints on the large-x gluon PDF*, *JHEP* **1402** (2014) 126, [arXiv:1311.1810].

[153] J. Butterworth, G. Dissertori, S. Dittmaier, D. de Florian, N. Glover, et al., *Les Houches 2013: Physics at TeV Colliders: Standard Model Working Group Report*, arXiv:1405.1067.

[154] J. Rojo et al., "Chapter 22 in: J. R. Andersen et al., "The SM and NLO multileg working group: Summary report"." arXiv:1003.1241, 2010.